Graduate Theses, Dissertations, and Problem Reports

2020

Cu-Based Electrocatalysts for Carbon Dioxide Conversion to Value-Added Chemicals

Qingyang Li
ql0012@mix.wvu.edu

Follow this and additional works at: https://researchrepository.wvu.edu/etd

Part of the Catalysis and Reaction Engineering Commons

Cu-Based Electrocatalysts for Carbon Dioxide Conversion to Value-Added Chemicals

Qingyang Li

Problem Report submitted to

the Statler College of Engineering and Mineral Resources

at West Virginia University

in partial fulfillment of the requirements for the degree of

Master of Science

in

Chemical Engineering

Jianli (John) Hu, Ph.D., Committee Chair

Charter Stinespring, Ph.D.

Debangsu Bhattacharyya, Ph.D.

Department of Chemical and Biomedical Engineering

Morgantown, West Virginia

2020

ABSTRACT

Cu-Based Electrocatalysts for Carbon Dioxide Conversion to Value-Added Chemicals

Qingyang Li

Massive usage of fossil fuel has being causing considerable emission of CO_2, which increases the temperature of the planet and greatly threaten human living environment, such as soil degradation, lower agricultural productivity, desertification, less biodiversity, fresh-water reduction, ocean acidification, ozone sphere destruction, etc. A number of technologies are being developed to reduce the CO_2 amount, however, all existing technologies except utilizing CO_2 as a feedstock, are hardly to essentially close the anthropogenic carbon loop. Currently, considering the economy and operability, electroreduction of CO_2 seems to be the most promising strategy to convert CO_2 to high value chemicals.

During the process of CO_2 electroreduction, Cu-based catalysts become the most popular because they meet the requirements of activating CO_2 and intermediates, suppression of hydrogen formation, and electron transportation. Herein, the factors that affect the Cu-based catalysts' performance, including morphology, particle sizes, presence of atomic-scale defects, surface roughness, residual oxygen atoms, and so on, have been surveyed and discussed. In addition, the most probable reaction pathways to synthesize the desirable C_2 products under different situation have been identified, which follow *CO + *CO → *COCO, *CO + *COH → C_2, *CO + *CHO → C_2 and *COH → *CH$_2$ → C_2. This report will benefit the design and optimization of Cu-based catalysts for the conversion of CO_2 to high value chemicals with high efficiency and selectivity.

Acknowledgements

I have been encouraged by many people along the journey of my MS studies over the past three years.

I would like to first express my sincerest gratitude and appreciation to my advisor, Dr. John Hu, for his guidance and encouragement during this work. He is my mentor for both his knowledge and personality.

I also would like to thank Dr. Debangsu Bhattacharyya for his patience and invaluable suggestions on my thesis.

I must especially thank Dr. Charter Stinespring. He taught me three courses and guided me during the MS program.

I am grateful to Dr. John W. Zondlo, Dr. Rakesh K. Gupta, Dr. Richard Turton, Dr. Hanjing Tian, Dr. Xueyan Song, Dr. David J. Klinke, Dr. Jeremy S. Hardinger, Dr. Xinjian He and Dr. Xiaopeng Ning for their teaching and kindness.

I am thankful to all graduate students, especially Ashley Caiola and I-Wen Wang, in the Department of Chemical Engineering for their friendliness, warmth and help that have made my stay in Morgantown pleasant and productive.

Finally, thanks to my family members. Throughout my life, they have supported me with unconditional love and care. They always believe in me and encourage me to be a better person.

Table of Contents

List of abbreviations (Alphabetical):

Abbreviation	Full Name
ADF	Annular dark-field
DAT	3,5-diamino-1,2,4-triazole
DFT	Density functional theory
EDS/ EDX	Energy dispersive X-ray spectroscopy
EEL	Electron energy loss
FE	Faradaic efficiency
FT	Fischer-Tropsch
GCP	Global Carbon Project
HER	Hydrogen evolution reaction
Hupd	Hydrogen underpotential deposition
NA	Nanoalloys
NC	Nanocubes
NP	Nanoparticles
NPS	National Park Service
NS	Nanosheets
NW	Nanowires
OLEMS	Online electrochemical mass spectrometry
PorCu	Copper-porphyrin
RDS	Rate-determining steps
RHE	Reversible hydrogen electrode
SEM	Scanning electron microscope
SHE	Standard hydrogen electrode
STEM	Scanning transmission electron microscope
TEM	Transmission electron microscope
TPD-MS	Temperature Programmed Desorption Mass Spectrometry
TPR	Temperature programmed reduction
XPS	X-ray photoelectron spectroscopy
XRD	X-ray diffraction

List of figures, tables and schemes:

Chapter 1. Introduction

Greenhouse gases are mainly composed of carbon dioxide (CO_2), carbon monoxide (CO), nitrogen oxides (NOx), methane (CH_4) and fluorinated gases, making much contribution to sustain the earth's temperature for the reason that greenhouse gases can absorb thermal radiation from the earth's surface and then re-emits the radiation back to the earth (Figure 1.1). However, continuously increasing greenhouse gases have being dramatically increasing the temperature of our planet due to massive usage of fossil fuel and other industrial activities in which produced considerable emission of CO_2, NOx, hydrocarbons, CO, and so on (Figure 1.2). Rising temperature may cause soil degradation, lower agricultural productivity, desertification, less biodiversity, fresh-water reduction, ozone sphere destruction, etc. Excessive greenhouse gases also have a directly negative effect on human living environment, such as natural disasters, malnutrition, and increased mortality induced by heat wave [1-3].
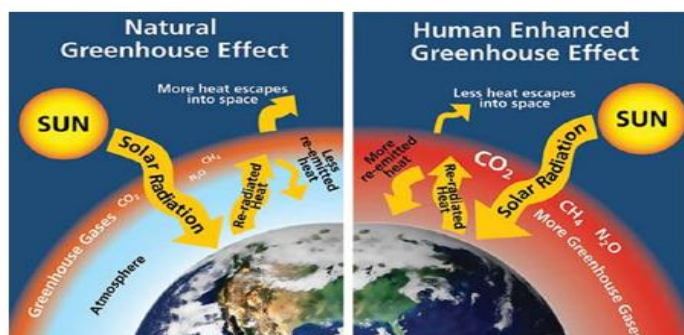
Figure.1.1 Greater concentrations of greenhouse gases mean more solar radiation is trapped within the Earth's atmosphere, making temperatures rise. Source: W. Elder, NPS
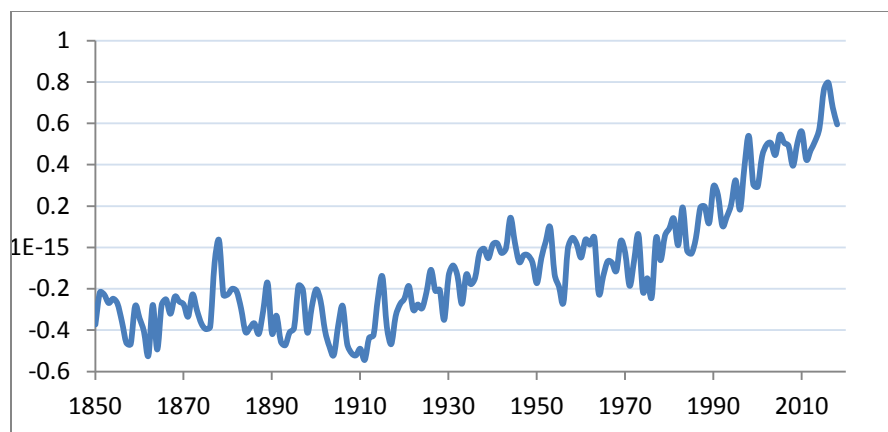
Figure.1.2 Global average land-sea temperature anomaly relative to the 1961-1990 average temperature in degrees celsius (°C). Source: Hadley Center (Had CRUT4).

Notably, CO_2, accounting for nearly 77% of greenhouse gases, has extremely increased after industrial revolution and should be principally responsible for global warming [4,5]. Before industrial revolution, new-produced CO_2 can be consumed by plants to keep the concentration of CO_2 balanced. In recent years, it is clearly realized that the human-generated CO_2 greatly exceeds the threshold of nature's capability (Table1.1). It is reported by Global Carbon Project (GCP) that global CO_2 emission from burning fossil fuels, the culprit of CO_2 emission, increased by 2.7 percent in 2018, after a 1.6 percent increase in 2017.

Table 1.1. Increase of carbon dioxide in the atmosphere for the last 1000 years [2,3].

Year	Period (year)	Concentration (ppm)	Increase (ppm)	Increase rate (ppm/year)
1000-1800	800	270-280	10	0.01
1800-1950	150	280-310	30	0.2
1958-1975	17	315-330	15	0.9
1975-2002	27	330-370	40	1.5 (8 billion tons)
2002-2010	8	370-388	18	2.25 (12 billion tons)
2010-2018	8	388-407	19	2.38

In the past decades, people gradually realized the significance and urgency of controlling CO_2 concentration to prevent the Earth's temperature from continuously increasing. Though relative methods and research are conducted to solve those problems, the effect is limited and the CO_2 concentration continues to grow [6,7]. Therefore, many nations, especially those main emission countries, have issued more strict laws and taken more actions to reverse the situation. For example, in 2011, the US Department of Energy (DOE) invested \$106 million in various CO_2-utilization projects, and in 2018, DOE invested \$17.6 millions and \$44 millions in Technologies Capable of Reducing CO_2 Capture Cost and Energy Penalties, and Advanced Carbon Capture Technologies Projects, respectively. In addition, the European Union has set up a prize worths €1.5 million for a technology demonstrating viable CO_2 utilization in 2020. China is expected to invest \$4-5 billion in CO_2 recycling from main emission sources, such as coal, steel, cement and paper industries [8-10].

Based on the previous and current supports from society and governments, technologies are being developed and applied to further solve the problems. In the following chapters, these technologies will be discussed in detail.

Reference

[1] Rossati, A. (2017). Global warming and its health impact. Int J Occup Environ Med (The IJOEM), 8(1 January), 963-7.

[2] Labonté, R., Mohindra, K., & Schrecker, T. (2011). The growing impact of globalization for health and public health practice. Annual review of public health, 32.

[3] Solow, A. R. (2013). Global warming: A call for peace on climate and conflict. Nature, 497(7448), 179.

[4] Köne, A. Ç., & Büke, T. (2010). Forecasting of CO_2 emissions from fuel combustion using trend analysis. Renewable and Sustainable Energy Reviews, 14(9), 2906-2915.

[5] Lindsey, R. (2018). Climate change: atmospheric carbon dioxide. National Oceanographic and Atmospheric Administration, News & Features. August.

[6] Omae, I. (2016). Carbon Dioxide Utilization by the Five-Membered Ring Products of Cyclometalation Reactions. Current organic chemistry, 20(9), 953.

[7] Greenwood, N. N., & Earnshaw, A. (2012). Chemistry of the Elements. Elsevier.

[8] Carbon Capture and Storage News. https://www.energy.gov/fe/listings/carbon-capture-and-storage-news

[9] Commission launches three Horizon Prizes for energy innovation. https://ec.europa.eu/programmes/horizon2020/en/news/commission-launches-three-horizon-prizes-energy-innovation

[10] Lim, X. (2015). How to make the most of carbon dioxide. Nature News, 526(7575), 628.

Chapter 2. Current technologies and on-going research for CO_2 treatment

Introduction

CO_2 is generated from both nature and human activities. Natural sources are composed of decomposition, ocean release and respiration, while human activities include cements and papers production, deforestation, and burning of fossil fuel, etc. Basically, there are two ways to control and even reduce the CO_2 concentration: 1) replacing the traditional fossil fuel, which accounts for 87 percent of all human-produced CO_2 emissions, with renewable clean energy, such as solar, wind and bioenergy; 2) capturing, sequestration and utilization of CO_2 [1-3]. Here, we will focus on the second method. Although the concentration of CO_2 has dramatically increased in past decades, its absolute concentration in the air is still low at about 0.04% [4-6]. Therefore, the first challenge is to capture diluted CO_2 in the air. After CO_2 is captured, it can be sequestrated or utilized as a feedstock to produce chemicals or fuels.

2.1 Carbon dioxide capture

In order to utilize carbon dioxide, the first step is to capture it efficiently. In theory, CO_2 even at low concentration can be transported and injected underground, however, energy cost and other associated costs make this approach impractical [7-9]. Therefore, pure CO_2 needs to be produced for the purpose of transportation and storage. CO_2 capture requires the separation of CO_2 from other species contained in industrial gases, such as flue gas, synthetic gas, air, or raw natural gas [10,11]. These separation steps can be accomplished by physical or chemical solvents, filtration membranes, solid adsorbents, or cryogenic separation. There are two approaches to

collect CO_2 with high concentration: 1) capture it from the large emission factories, utility plant, steel and cement plants; 2) and collect it directly in the atmosphere [12,13].

2.1.1 Capture CO_2 from industrial sources

Basically, there are three different technologies that can be used to capture CO_2 from the large industrial sources as shown in Figure 2.1, including post-combustion, pre-combustion, and oxyfuel. Post-combustion approach separates CO_2 from the flue gas produced by the primary fuel combustion in the air [14-16]. In pre-combustion approach, fuel reacts with steam and air or oxygen first to produce syngas (CO and H_2). Then, CO is converted to CO_2 by further reaction with steam via water-gas-shift reaction, and H_2 is separated as fuel. In this process, a lot of work needs to be done in the early stage, but the separation is relatively easier in the later stage, and hydrogen can be utilized in many industrial processes. Oxy-fuel system uses oxygen to substitute air for primary combustion, producing flue gases dominated by water vapor and CO_2. This process requires the separation of oxygen from the air first. The flue gas produced by this method has a very high concentration of CO_2 [17-20]. It is economically feasible to capture CO_2 in power plants with post-combustion system under certain conditions. CO_2 separation from natural gas is a matured technology. The technology of pre-combustion has been widely used in the fertilizer manufacturing and hydrogen production industries.
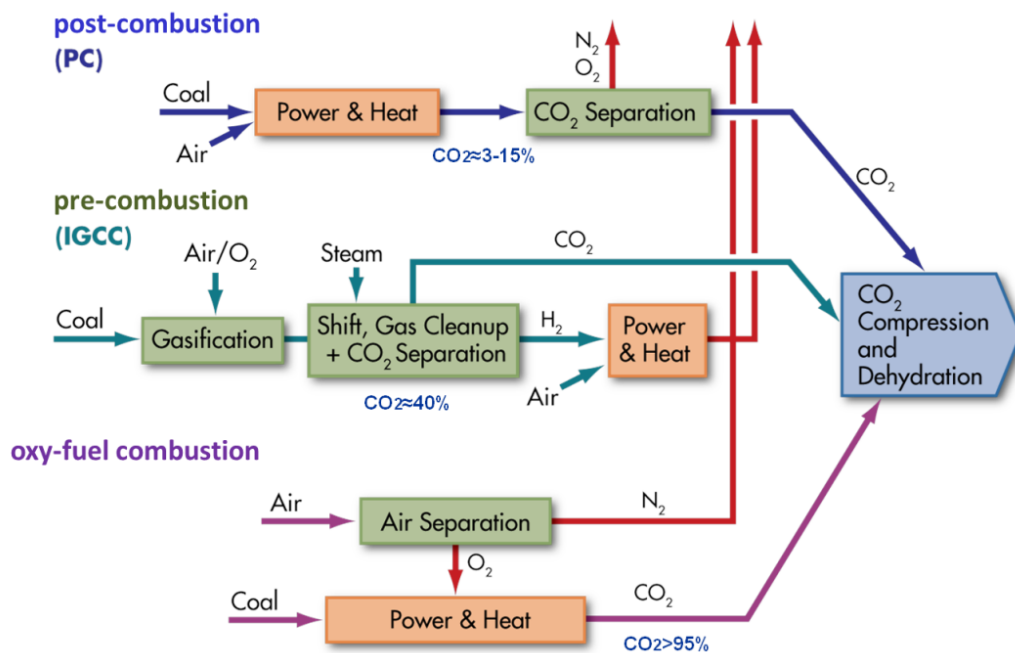
Figure 2.1. Summary of CO_2 capture technologies [18].

Organic solvent and membrane are usually used to separate and capture CO_2. Normally, organic solvents, such as monoethanolamine (MEA) and ammonia, are considered as the most available and widely used technology. However, it is not reasonable to considered it as a sustainable technology for its high cost and difficulty in regeneration. Membrane technology will be one of the most promising technologies, because it is compact, modular, mobile, low cost and environment-friendly [21-25].

2.1.2 Capture CO_2 from atmosphere

Chemically scrubbing CO_2 directly from the ambient air is another technology for CO_2 capture [26]. Though it is costly and energy-intensive, it is still an attractive technology because its potential scale of deployment is enormous [27-29].

2. 2 CO_2 storage and sequestration

CO_2 sequestration is considered as a potential technology for large-scale reduction of CO_2 concentration in the air. The idea is to inject compressed CO_2 into the ground or ocean to store it there for a long period of time [30-32]. For oceanic fixation, liquid carbon dioxide is injected into the ocean at different depths via ocean pipelines or marine transportation vessels, allowing it to dissolve in water or form stable carbon dioxide lakes. On land, liquid carbon dioxide is injected into the underground formation where it is locked by water dissolution, physical adsorption or chemical reactions (Figure 2.2).

In 2013, the United States Geological Survey (USGS) released the first comprehensive, geologically-based probabilistic assessment for CO_2, showing a range of 2,400 to 3,700 metric gigatons of potential CO_2 storage in USA. In addition, assessment also proved that carbon dioxide can be successfully injected using today's engineering practices and technologies [33,34]. However, Geological and oceanic sequestration have significant disadvantages. For example, when CO_2 is injected into the ocean, it may lead to the acidification of seawater, endangering the ecosystem. In addition, there is a risk of leakage that could contaminate groundwater or endanger organisms after it is buried underground. In the past, sequestration of CO_2 in the underground was practiced for its convenience and low cost. However, in recent years, the social acceptance becomes lower and lower for the uncertainty and controversy [35,36].
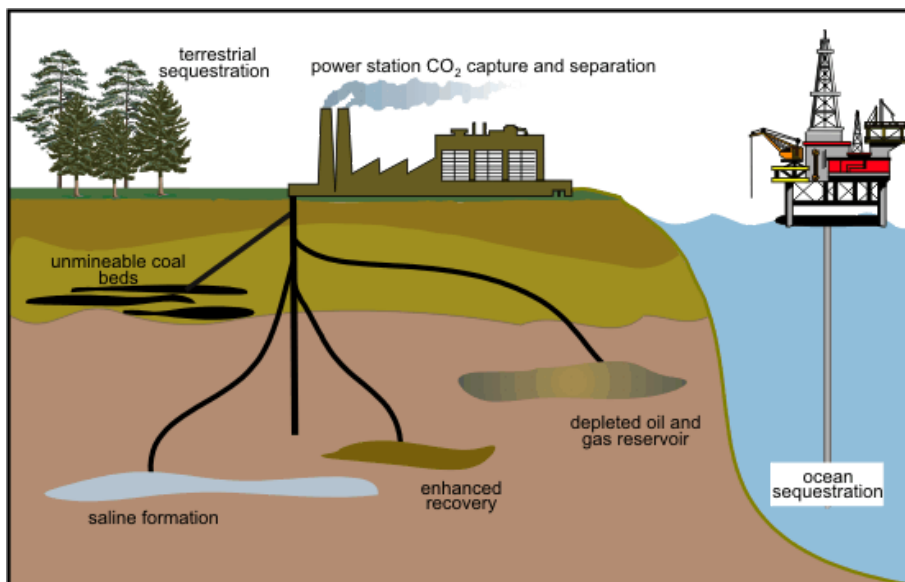
Figure 2.2. CO_2 sequestration underground and in sea. Source: Reagan Smith Energy Solutions, INC.

2.3 CO_2 utilization

According to the report from Energy Information Administration (EIA), in the coming decades, energy consumption will increase continuously and fossil fuel still dominates the energy market, which means CO_2 emission will further threaten our lives (Figure 2.3). Closing material cycle is a fundamental principle of industrial ecology. Hence, the best way to avoid sustained CO_2 increase in the atmosphere is to keep the carbon balanced in biosphere [37-40]. Obviously, CO_2 utilization is more consistent with this principle than CO_2 sequestration. Basically, there are two ways to utilize CO_2: 1) use it "as is"; 2) used it as feedstock to synthesize fuels and chemicals.
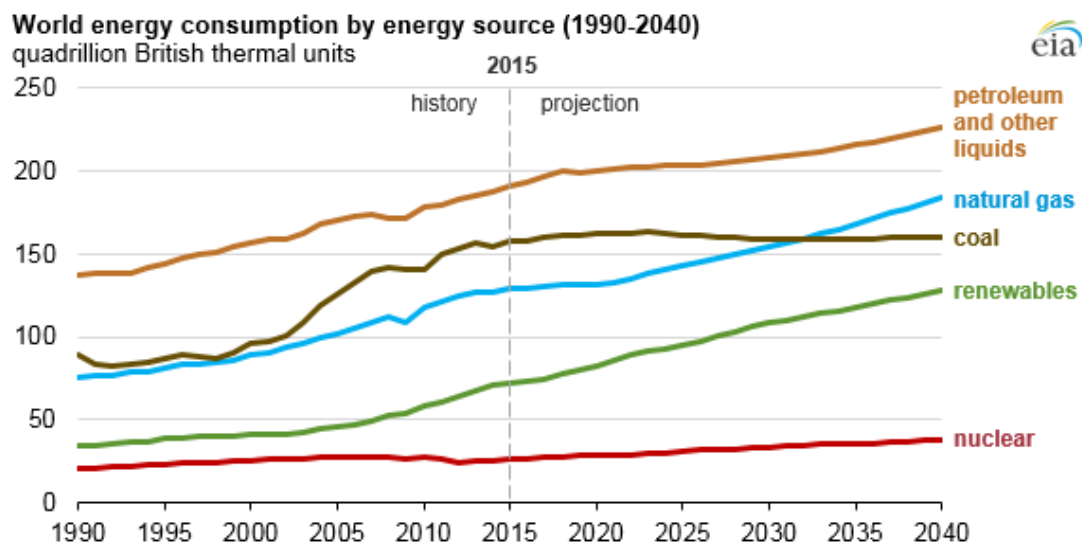
Figure 2.3. World energy consumption tendency. Source: U.S. Energy Information Administration, International Energy Outlook 2017.

2.3.1 Use CO_2 "as is"

Every year, about 20 million tonnes of CO_2 are widely utilized in industries "as is" [41]. For example, it is used as shield gas in manufacturing and construction industries at a large scale. In food industry, people use it to prevent fungal and bacterial growth, carbonate soft drinks, beers and wine, de-caffeinate coffee, keep food fresh, etc [42,43]. In oilfield, engineers use CO_2 foam to enhance oil recovery. Interestingly, CO_2 can be captured to enhance the growth of plants as some studies have shown that increasing the concentration of CO_2 appropriately is beneficial to photosynthesis [44]. In addition, it is also used for neutralizing alkaline water, and producing fire extinguishers.

2.3.2 CO_2 is used as feedstock for chemical synthesis

Statistically, over 90% of commercially available organic chemicals are produced from crude oil. CO_2 conversion to organic chemicals will help reduce the emitted CO_2 in air and the consumption of petroleum. In reality, industry has made some progress in utilizing CO_2 as raw

materials to produce chemicals (Table 2.1). Two notable examples are salicylic acid and urea

produced from CO_2 which account for approximately 60% of the total worldwide consumption.

Table 2.1. Major commodity chemicals currently synthesized from CO_2 on an industrial scale
globally. First three groups data are cited from reference [45] and the other data are cited from
reference [46].

Chemical	Production (ton)
Cyclic carbonates	80,000 in 2010
Salicylic acid	89,800 in 2013
Urea	164,000,000 in 2015
Polycarbonate (Asahi Kasei process)	605,000
Polypropylene carbonate	76,000
Acetylsalicylic acid	90,000
Methanol	4000

Thanks to the advances in technology, more and more methods for CO_2 utilization have

been developed in recent decades. For example, since 2013, Calera has been using CO_2 to

produce pure calcium carbonate, which is turned into fiber cement boards [47,48]. More research

has being conducted to convert CO_2 to cyclic carbonates due to its rapid growth in the area of

electrolytes for lithium ion batteries [49,50]. Another promising area is the production of polyols,

which are used as the raw material for polymers to further produce adhesives, coatings,

mattresses, insulation refrigerator, and so on.

2.3.3 CO_2 conversion to fuel

People have been debating the unmeaning topic for several decades when fossil energy will

run out. First, it is hard to predict the amount of fossil fuel because it is subjected to many

uncertain factors, such as the development of exploration and exploitation technology, and the

consumption rate. Second, the environment cannot enduringly tolerate the use of fossil as the

main energy source and the energy configuration must be changed because fossil energy will

inevitably cause global warming, acid rain, haze, and so on. Therefore, establishing a renewable

carbon system will not only reduce CO_2 emissions, but also alleviate other pollution caused by

fossil processing and transportation. Though tremendous work has been done to convert CO_2 to

high-value products, it is impossible to essentially close the anthropogenic carbon loop. Because

about 70% fossil fuel is combusted to generate energy while only 7% is used as chemical

products according to the data from EIA (Figure 2.4). Therefore, to prevent continuous carbon

accumulation in ecosphere, fossil fuel must be replaced by other energy without carbon emission,

such as solar, wind and water.
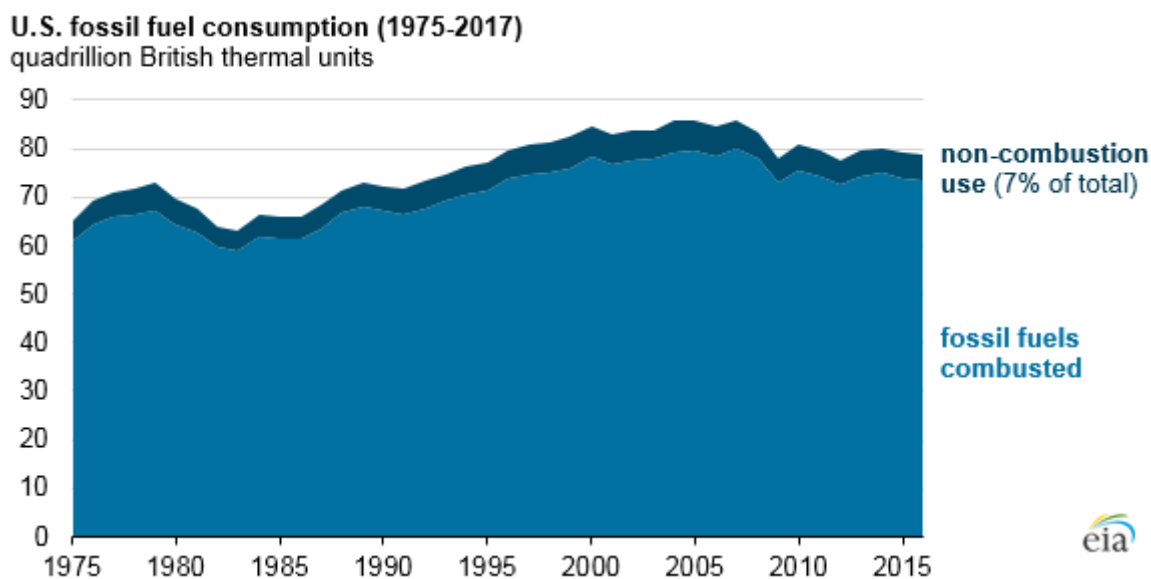
Figure 2.4. Usage pattern of US fossil fuel. Source: U.S. Energy Information
Administration, Monthly Energy Review.

    Reduction of CO_2 to fuel has become the most promising strategy because it helps reduce

the amount of CO_2 in air and CO_2 can work as an energy storage matrix where other energy can

be stored and transported. At least six potential CO_2 conversion technologies are current topics to

realize 3E (efficiency, effect and economy) and implement on industrial scale. Some of them are

close to commercialization, some are at the benchtop scale, and some have yet to be

scientifically proven (Figure 2.5).
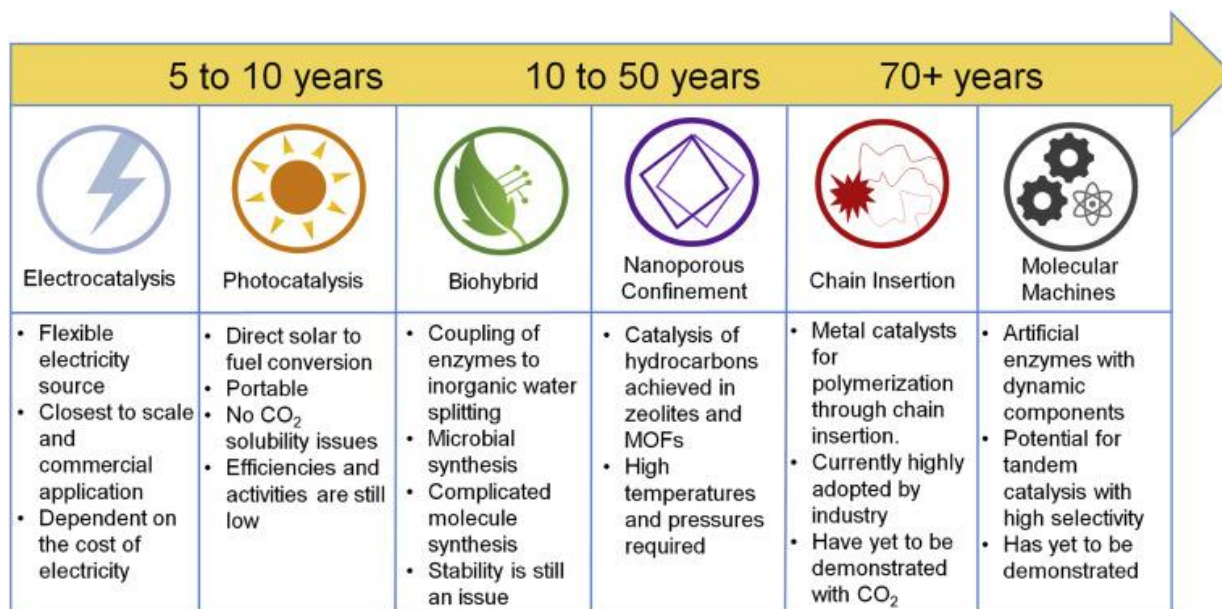
Figure 2.5. Proposed timeline of CO_2 utilization methods [54]. Note: the specific time ranges are based on extrapolation of timeline development of other disruptive technologies such as the advent of 3D printing, solar energy adoption, and electric vehicle development.

Electrocatalytic conversion of CO_2 is closest to commercialization [51-53]. Many startup

and established companies, such as Opus-12, Mitsui Chemicals, Carbon Recycling International,

and Carbon Electrocatalytic Recycling Toronto, are currently at the forefront to monetize the

technology [54,55]. With the cost decrease of renewable energy, electrocatalysis will become

more and more attractive [56].

However, CO_2 is extremely stable due to the strong C=O double bond with bonding energy

of 750 kJ mol^{-1} which is considerably larger than that of C-C (336 kJ mol^{-1}), C-O (327

kJ mol^{-1}), and C-H (411 kJ mol^{-1}) [57]. Significant energy is required to break the C=O bond.

Meanwhile, it is very difficult to control the reaction paths and lots of products may be produced

during the reduction process, increasing the difficulty in products separation (Table 2.3).

13

Table 2.3. Standard electrochemical potentials for CO_2 reduction [58].

Reduction potentials of CO_2	$E°$ [V] vs SHE at pH 7
$CO_2 + e^- \rightarrow CO_2^-$	−1.9
$CO_2 + 2H^+ + 2e^- \rightarrow HCOOH$	−0.61
$CO_2 + 2H^+ + 2e^- \rightarrow CO + H_2O$	−0.52
$2CO_2 + 12H^+ + 12e^- \rightarrow C_2H_4 + 4H_2O$	−0.34
$CO_2 + 4H^+ + 4e^- \rightarrow HCHO + H_2O$	−0.51
$CO_2 + 6H^+ + 6e^- \rightarrow CH_3OH + H_2O$	−0.38
$CO_2 + 8H^+ + 8e^- \rightarrow CH_4 + 2H_2O$	−0.24
$2H^+ + 2e^- \rightarrow H_2$	−0.42

The foreground of CO_2 reduction for commercial use is dependent on the development of highly efficient and selective catalysts with relatively low energy cost. In recent years, much progress have been made on catalyst to reduce the energy barrier and control reaction pathway [59,60]. In the coming chapter, we will focus on the most popular catalysts, Cu-based catalysts, and summarize the factors influencing their performance.

Reference

[1] Shahbazi, A., & Nasab, B. R. (2016). Carbon capture and storage (CCS) and its impacts on climate change and global warming. J. Pet. Environ. Biotechnol, 7, 291.

[2] Fang, C., Wang, S., & Li, G. (2015). Changing urban forms and carbon dioxide emissions in China: A case study of 30 provincial capital cities. Applied energy, 158, 519-531.

[3] Hunt, A. J., Sin, E. H., Marriott, R., & Clark, J. H. (2010). Generation, capture, and utilization of industrial carbon dioxide. ChemSusChem: Chemistry & Sustainability Energy & Materials, 3(3), 306-322.

[4] Eiler, J. M., & Schauble, E. (2004). 18O13C16O in Earth's atmosphere. Geochimica et Cosmochimica Acta, 68(23), 4767-4777.

[5] Pielke Jr, R. A. (2009). An idealized assessment of the economics of air capture of carbon dioxide in mitigation policy. environmental science & policy, 12(3), 216-225.

[6] Köne, A. Ç., & Büke, T. (2010). Forecasting of CO_2 emissions from fuel combustion using trend analysis. Renewable and Sustainable Energy Reviews, 14(9), 2906-2915.

[7] Rubin, E. S., Davison, J. E., & Herzog, H. J. (2015). The cost of CO_2 capture and storage. International Journal of Greenhouse Gas Control, 40, 378-400.

[8] Rubin, E., Meyer, L., & Coninck, H. (2005). Carbon Dioxide Capture and Storage, Technical Summary. IPCC special report, 29.

[9] Change, I. P. O. C. (2014). IPCC. Climate change.

[10] McDonald, T. M., Lee, W. R., Mason, J. A., Wiers, B. M., Hong, C. S., & Long, J. R. (2012). Capture of carbon dioxide from air and flue gas in the alkylamine-appended metal–organic framework mmen-Mg2 (dobpdc). Journal of the American Chemical Society, 134(16), 7056-7065.

[11] Baker, R. W. (2002). Future directions of membrane gas separation technology. Industrial & engineering chemistry research, 41(6), 1393-1411.

[12] Bhown, A. S., & Freeman, B. C. (2011). Analysis and status of post-combustion carbon dioxide capture technologies. Environmental science & technology, 45(20), 8624-8632.

[13] Jansen, D., Gazzani, M., Manzolini, G., van Dijk, E., & Carbo, M. (2015). Pre-combustion CO_2 capture. International Journal of Greenhouse Gas Control, 40, 167-187.

[14] Wang, Y., Zhao, L., Otto, A., Robinius, M., & Stolten, D. (2017). A review of post-combustion CO_2 capture technologies from coal-fired power plants. Energy Procedia, 114, 650-665.

[15] Shakerian, F., Kim, K. H., Szulejko, J. E., & Park, J. W. (2015). A comparative review between amines and ammonia as sorptive media for post-combustion CO_2 capture. Applied Energy, 148, 10-22.

[16] Wang, M., Joel, A. S., Ramshaw, C., Eimer, D., & Musa, N. M. (2015). Process intensification for post-combustion CO_2 capture with chemical absorption: a critical review. Applied Energy, 158, 275-291.

[17] Rahman, F. A., Aziz, M. M. A., Saidur, R., Bakar, W. A. W. A., Hainin, M. R., Putrajaya, R., & Hassan, N. A. (2017). Pollution to solution: Capture and sequestration of carbon dioxide (CO2) and its utilization as a renewable energy source for a sustainable future. Renewable and Sustainable Energy Reviews, 71, 112-126.

[18] Llamas, B., Navarrete, B., Vega, F., Rodriguez, E., Mazadiego, L. F., Cámara, Á., & Otero, P. (2016). Greenhouse Gas Emissions-Carbon Capture, Storage and Utilisation. Greenhouse Gases, 81.

[19] Jansen, D., Gazzani, M., Manzolini, G., van Dijk, E., & Carbo, M. (2015). Pre-combustion CO_2 capture. International Journal of Greenhouse Gas Control, 40, 167-187.

[20] Buhre, B. J., Elliott, L. K., Sheng, C. D., Gupta, R. P., & Wall, T. F. (2005). Oxy-fuel combustion technology for coal-fired power generation. Progress in energy and combustion science, 31(4), 283-307.

[21] Toftegaard, M. B., Brix, J., Jensen, P. A., Glarborg, P., & Jensen, A. D. (2010). Oxy-fuel combustion of solid fuels. Progress in energy and combustion science, 36(5), 581-625.

[22] Aaron, D., & Tsouris, C. (2005). Separation of CO_2 from flue gas: a review. Separation Science and Technology, 40(1-3), 321-348.

[23] Yang, H., Xu, Z., Fan, M., Gupta, R., Slimane, R. B., Bland, A. E., & Wright, I. (2008). Progress in carbon dioxide separation and capture: A review. Journal of environmental sciences, 20(1), 14-27.

[24] Dumée, L., Scholes, C., Stevens, G., & Kentish, S. (2012). Purification of aqueous amine solvents used in post combustion CO_2 capture: A review. International Journal of Greenhouse Gas Control, 10, 443-455.

[25] Meylan, F. D., Moreau, V., & Erkman, S. (2015). CO_2 utilization in the perspective of industrial ecology, an overview. Journal of CO_2 Utilization, 12, 101-108.

[26] Keith, D. W., Holmes, G., Angelo, D. S., & Heidel, K. (2018). A Process for Capturing CO_2 from the Atmosphere. Joule, 2(8), 1573-1594.

[27] Lackner, K. S. (2009). Capture of carbon dioxide from ambient air. The European Physical Journal Special Topics, 176(1), 93-106.

[28] Lackner, K. S., Brennan, S., Matter, J. M., Park, A. H. A., Wright, A., & Van Der Zwaan, B. (2012). The urgency of the development of CO_2 capture from ambient air. Proceedings of the National Academy of Sciences, 109(33), 13156-13162.

[29] House, K. Z., Baclig, A. C., Ranjan, M., van Nierop, E. A., Wilcox, J., & Herzog, H. J. (2011). Economic and energetic analysis of capturing CO_2 from ambient air. Proceedings of the National Academy of Sciences, 108(51), 20428-20433.

[30] Randolph, J. B., & Saar, M. O. (2011). Coupling carbon dioxide sequestration with geothermal energy capture in naturally permeable, porous geologic formations: Implications for CO_2 sequestration. Energy Procedia, 4, 2206-2213.

[31] Woodrow, H. (2013, September). Exergy Analysis of Coupled CO_2 Sequestration with Geothermal Energy Production. In Second EAGE Sustainable Earth Sciences (SES) Conference and Exhibition.

[32] uadrelli, E. A., Centi, G., Duplan, J. L., & Perathoner, S. (2011). Carbon dioxide recycling: emerging large-scale technologies with industrial potential. ChemSusChem, 4(9), 1194-1215.

[33] Pires, J. C. M., Martins, F. G., Alvim-Ferraz, M. C. M., & Simões, M. (2011). Recent developments on carbon capture and storage: an overview. Chemical engineering research and design, 89(9), 1446-1460.

[34] Leung, D. Y., Caramanna, G., & Maroto-Valer, M. M. (2014). An overview of current status of carbon dioxide capture and storage technologies. Renewable and Sustainable Energy Reviews, 39, 426-443.

[35] Little, M. G., & Jackson, R. B. (2010). Potential impacts of leakage from deep CO_2 geosequestration on overlying freshwater aquifers. Environmental science & technology, 44(23), 9225-9232.

[36] Zoback, M. D., & Gorelick, S. M. (2012). Earthquake triggering and large-scale geologic storage of carbon dioxide. Proceedings of the National Academy of Sciences, 109(26), 10164-10168.

[37] Budzianowski, W. M. (2012). Value-added carbon management technologies for low CO_2 intensive carbon-based energy vectors. Energy, 41(1), 280-297.

[38] Yi, Q., Li, W., Feng, J., & Xie, K. (2015). Carbon cycle in advanced coal chemical engineering. Chemical Society Reviews, 44(15), 5409-5445.

[39] Ciais, P., Bombelli, A., Williams, M., Piao, S. L., Chave, J., Ryan, C. M., ... & Valentini, R. (2011). The carbon balance of Africa: synthesis of recent research studies. Philosophical transactions of the royal society A: Mathematical, Physical and Engineering Sciences, 369(1943), 2038-2057.

[40] Engström, K., Lindeskog, M., Olin, S., Hassler, J., & Smith, B. (2017). Impacts of climate mitigation strategies in the energy sector on global land use and carbon balance. Earth System Dynamics, 8(3), 773.

[41] Lim, X. (2015). How to make the most of carbon dioxide. Nature News, 526(7575), 628.

[42] How the CO_2 shortage is affecting the food and drink industry. https://www.ft.com/content/36183d1e-7b73-11e8-bc55-50daf11b720d.

[43] Bui, M., Adjiman, C. S., Bardow, A., Anthony, E. J., Boston, A., Brown, S., ... & Hallett, J. P. (2018). Carbon capture and storage (CCS): the way forward. Energy & Environmental Science, 11(5), 1062-1176.

[44] Zheng, Y., Li, F., Hao, L., Shedayi, A. A., Guo, L., Ma, C., ... & Xu, M. (2018). The optimal CO_2 concentrations for the growth of three perennial grass species. BMC plant biology, 18(1), 27.

[45] National Academies of Sciences, Engineering, and Medicine. (2019). Gaseous Carbon Waste Streams Utilization: Status and Research Needs. National Academies Press.

[46] Omae, I. (2012). Recent developments in carbon dioxide utilization for the production of organic chemicals. Coordination Chemistry Reviews, 256(13-14), 1384-1405.

[47] Butler, J. N. (2019). Carbon dioxide equilibria and their applications. Routledge.

[48] Macartney, A., & Knops, P. (2019). 11 Mineral carbon sequestration. Fundamentals, 187.

[49] Kim, Y., Hyun, K., Ahn, D., Kim, R., Park, M. H., & Kim, Y. (2019). Efficient Aluminum Catalysts for the Chemical Conversion of CO_2 into Cyclic Carbonates at Room Temperature and Atmospheric CO_2 Pressure. ChemSusChem.

[50] Puthiaraj, P., Ravi, S., Yu, K., & Ahn, W. S. (2019). CO_2 adsorption and conversion into cyclic carbonates over a porous $ZnBr_2$-grafted N-heterocyclic carbene-based aromatic polymer. Applied Catalysis B: Environmental, 251, 195-205.

[51] Jiang, Z., Xiao, T., Kuznetsov, V. Á., & Edwards, P. Á. (2010). Turning carbon dioxide into fuel. Philosophical Transactions of the Royal Society A: Mathematical, Physical and Engineering Sciences, 368(1923), 3343-3364.

[52] Zhang, S., Kang, P., & Meyer, T. J. (2014). Nanostructured tin catalysts for selective electrochemical reduction of carbon dioxide to formate. Journal of the American Chemical Society, 136(5), 1734-1737.

[53] Creel, E. B., Corson, E. R., Eichhorn, J., Kostecki, R., Urban, J. J., & McCloskey, B. D. (2019). Directing Selectivity of Electrochemical Carbon Dioxide Reduction Using Plasmonics. ACS Energy Letters, 4(5), 1098-1105.

[54] Bushuyev, O. S., De Luna, P., Dinh, C. T., Tao, L., Saur, G., van de Lagemaat, J., ... & Sargent, E. H. (2018). What should we make with CO_2 and how can we make it?. Joule, 2(5), 825-832.

[55] Initiative, G. C. (2019). Global Roadmap for Implementing CO_2 Utilization. Global CO_2 Initiative.

[56] 2015 Wind Technologies Market Report. (2016). US Department of Energy.

[57] Wu, J., Huang, Y., Ye, W., & Li, Y. (2017). CO_2 reduction: from the electrochemical to photochemical approach. Advanced Science, 4(11), 1700194.

[58] Leitner, W. (1995). Carbon dioxide as a raw material: the synthesis of formic acid and its derivatives from CO_2. Angewandte Chemie International Edition in English, 34(20), 2207-2221.

[59] Kortlever, R., Shen, J., Schouten, K. J. P., Calle-Vallejo, F., & Koper, M. T. (2015). Catalysts and reaction pathways for the electrochemical reduction of carbon dioxide. The journal of physical chemistry letters, 6(20), 4073-4082.

[60] Kuhl, K. P., Cave, E. R., Abram, D. N., & Jaramillo, T. F. (2012). New insights into the electrochemical reduction of carbon dioxide on metallic copper surfaces. Energy & Environmental Science, 5(5), 7050-7059.

Chapter 3. Recent advances in CO_2 reduction on copper-based electrocatalysts

Introduction

Electrocatalysis is one of the most promising approaches for its renewable and environmental friendly properties as well as it has the potential to sustain solar-fuel-based economy. Many valuable products, such as CO, formate, methanol, methane, ethanol and ethylene, can be produced via electrocatalysis, which can be directly or indirectly used in industrial processes. For example, ethanol can be blended in gasoline for auto-engines, and CO can be converted to many chemicals via Fischer-Tropsch synthesis. Although it possesses great potential, the application is seriously held back by its high overpotential, poor selectivity and low faradaic efficiency. Therefore, it is urgent to study the reaction mechanism and develop tailor-made electrocatalysts.

The design of electrocatalytic reactor is critical in CO_2 reduction. Though many kinds of reactor configurations have been developed to enhance CO_2 conversion, the working principle is similar (Scheme 3.1). Typically, there are four main components in a reactor, including anode, cathode, membrane and electrolyte. Specifically, H_2O is oxidized to O_2 spilling at the anode, while CO_2 is electrochemically reduced to produce CO and low carbon organic compounds on the cathode, such as CH_3OH, CH_3CH_2OH, C_2H_4 and CH_4. According to the statistical data, platinum is commonly used as anode, and $KHCO_3$ dominates electrolyte field [3]. Many studies have reported improvement on the performance of membrane. Currently, Nafion produced by Dupont is the most popular one [4,5]. Multitudinous metals and their derivatives, such as Cu, Zn,

Ag, Au, Co, Pd, Bi, etc., are used as cathode. Scheme 3.2 details the structure and components of a electrochemical reactor [2].

In this chapter, we will discuss the progress in Cu-based catalysts because Cu is the most researched catalyst having the potential to be commercialized.
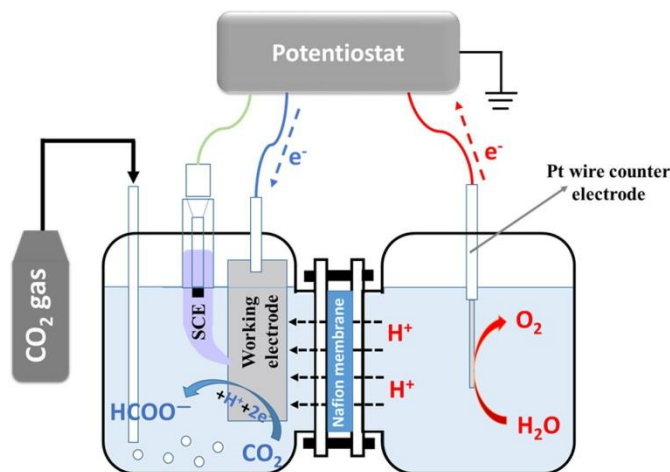
Scheme 3.1. Schematic illustration of electrochemical reduction of CO_2 [1].
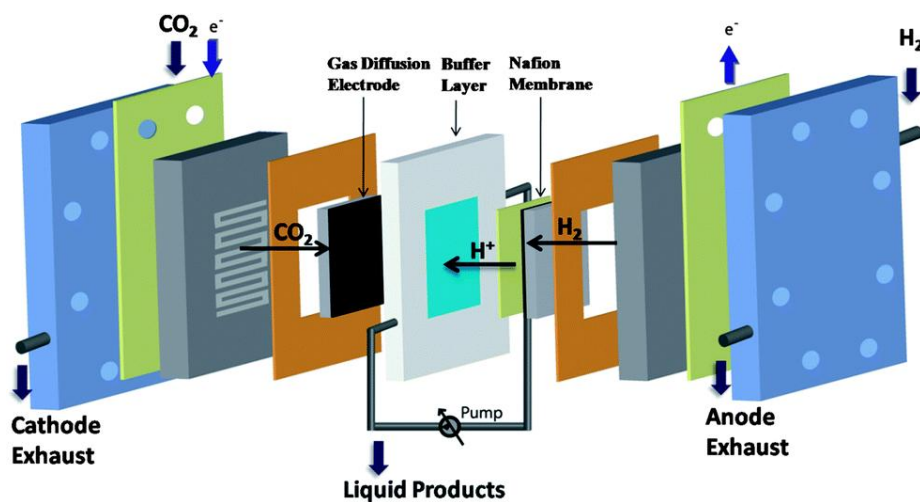
Scheme 3.2. A schematic drawing of the full electrochemical cell including a buffer layer with circulating liquid electrolyte [2].

The binding energies of *CO and *H (* denotes a surface adsorption site) are used as the descriptors for the correlation between the electrocatalytic performance and the surface property of different metals. It seems weak binding strength of *CO may cause massive CO formation because it is hard to absorb CO after it is formed on those metals, such us Au, Ag and Zn. While weak binding strength of *H may cause high proportion of H_2 because it is hard to absorb *H after it is formed on those metals, such as Ni and Pt. Among those metal catalysts, Cu possesses the intermediate binding strength to *CO and does not have hydrogen underpotential deposition (H_{upd}). Those are the reason why copper is the only metal producing various hydrocarbons with relative high efficiency (Figure 3.1 and Table 3.1). Currently, Cu is the most commonly studied and may be the most suitable for large-scale application due to its cheap price and excellent catalytic property [3,4].
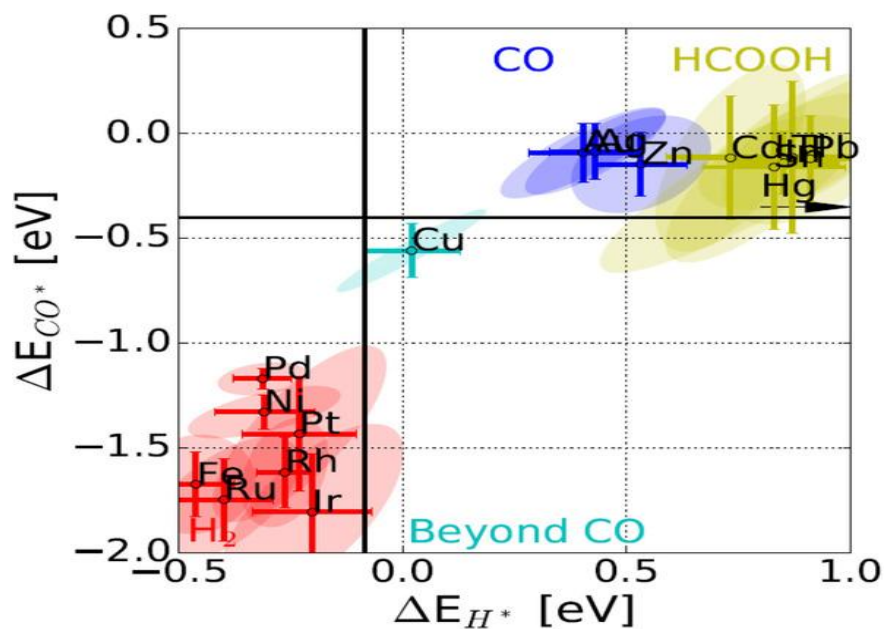
Figure 3.1. The binding energies of the intermediates, ΔE_{CO*} and ΔE_{H*}, (CO* = *CO, H* = *H) [3].

Table 3.1. Reported faradaic efficiencies of various products measured for the electroreduction of CO_2 in 0.1M $KHCO_3$ [4].

Electrode	Potential (V vs. SHE)	Current density (mA cm^{-2})	Faradaic efficiency (%)							
			CH$_4$	C$_2$H$_4$	C$_2$H$_6$O^b	C$_3$H$_8$O^c	CO	HCOO$^-$	H$_2$	Total
Pb	-1.63	5.0	0.0	0.0	0.0	0.0	0.0	97.4	5.0	102.4
Hg	-1.51	0.5	0.0	0.0	0.0	0.0	0.0	99.5	0.0	99.5
Tl	-1.60	5.0	0.0	0.0	0.0	0.0	0.0	95.1	6.2	101.3
In	-1.55	5.0	0.0	0.0	0.0	0.0	2.1	94.9	3.3	100.3
Sn	-1.48	5.0	0.0	0.0	0.0	0.0	7.1	88.4	4.6	100.1
Cd	-1.63	5.0	1.3	0.0	0.0	0.0	13.9	78.4	9.4	103.0
Bi	-1.56	1.2	-	-	-	-	-	77	-	-
Au	-1.14	5.0	0.0	0.0	0.0	0.0	87.1	0.7	10.2	98.0
Ag	-1.37	5.0	0.0	0.0	0.0	0.0	81.5	0.8	12.4	94.6
Zn	-1.54	5.0	0.0	0.0	0.0	0.0	79.4	6.1	9.9	95.4
Pd	-1.2	5.0	2.9	0.0	0.0	0.0	28.3	2.8	26.2	60.2
Ga	-1.24	5.0	0	0.0	0.0	0.0	23.2	0.0	79.0	102.0
Cu	-1.44	5.0	33.3	25.5	5.7	3.0	1.3	9.4	20.5	103.5
Ni	-1.48	5.0	1.8	0.1	0.0	0.0	0.0	1.4	88.9	92.4
Fe	-0.91	5.0	0.0	0.0	0.0	0.0	0.0	0.0	0.0	94.8
Pt	-1.07	5.0	0.0	0.0	0.0	0.0	0.0	0.1	95.7	95.8
Ti	-1.60	5.0	0.0	0.0	0.0	0.0	tr.	0.0	99.7	99.7

Though Cu looks like the best metal catalyst for electrocatalytic CO_2 reduction, its performance needs to be improved to achieve high efficiency and selectivity. As shown in Figure 3.2, under relative low potential of -0.75 V vs. RHE (Reversible Hydrogen Electrode), only H_2, CO and formate are produced [5]. According to previous research, the underlying reasons for high selectivity of Cu were related to local pH near electrode, morphology, particle sizes, the presence of atomic-scale defects, surface roughness, strains, and/or residual oxygen atoms in the catalysts, etc [6-9]. Experimental and computational results suggested that the active sites, chemical kinetics and transport effects greatly contributed to high efficiency and electivity. Here, we summarize the factors influencing the performance of Cu-based catalysts.
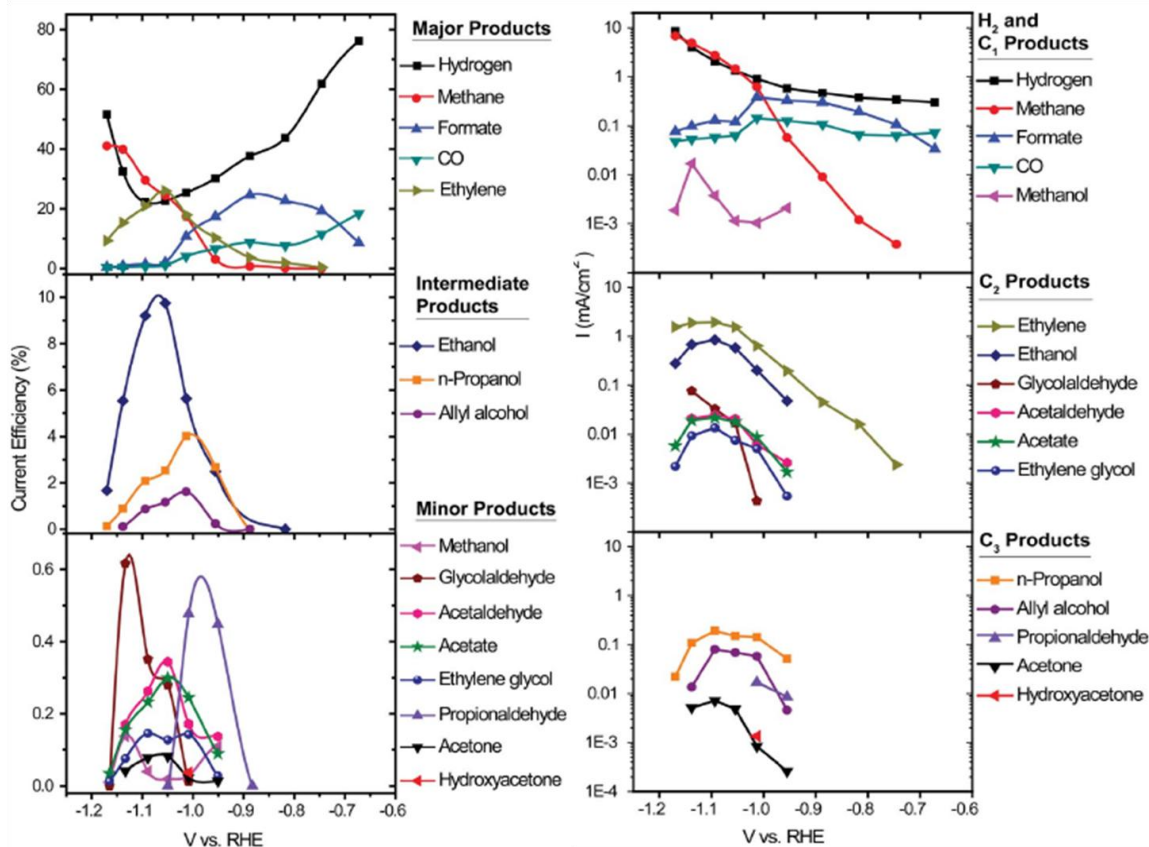
Figure 3.2. Current efficiency for each product as a function of potential (left) and Tafel plot of the partial current going to each product (right), respectively [5].

3.1 Fabricated Cu as the only metal for CO_2 conversion

3.1.1 The effects of current and potential

In 2018, Dan Ren et al[10] conducted a survey of the current and potential for CO_2 conversion, which showed the selectivity of $HCOO^-/CO$, C_2H_4, and CH_4 was greatly affected by current and potential as long as under the mass transport limitation of CO_2. Four Cu catalysts (metallic and oxide-derived) with different surface roughness were prepared via electrodeposition, termed as Cu-10, CuO-1, CuO-10, and CuO-60 with post-reduced roughness to be 1.4, 5, 48, and 186, respectively. The result showed that total current was positively related to the surface roughness and applied potential, while the maximum current for CO_2 reduction

23

was around -20 mA cm^{-2} when the total currents were around -40 mA cm^{-2} (Figure 3a). When the total current exceeded a particular value, the current density decreased and more H_2 was produced due to the low CO_2 concentration and buildup of OH^- near electrode (Figure 3b). It was proved that different energy barriers were the reason causing CO, $HCOO^-$, C_2H_4, C_2H_5OH, and CH_4 at different potential windows (Figures 3.3d-e). The morphology of Cu catalysts affected not only catalytic active sites, but also roughness for lying limiting current density in the suitable potential window for different products [11,12].
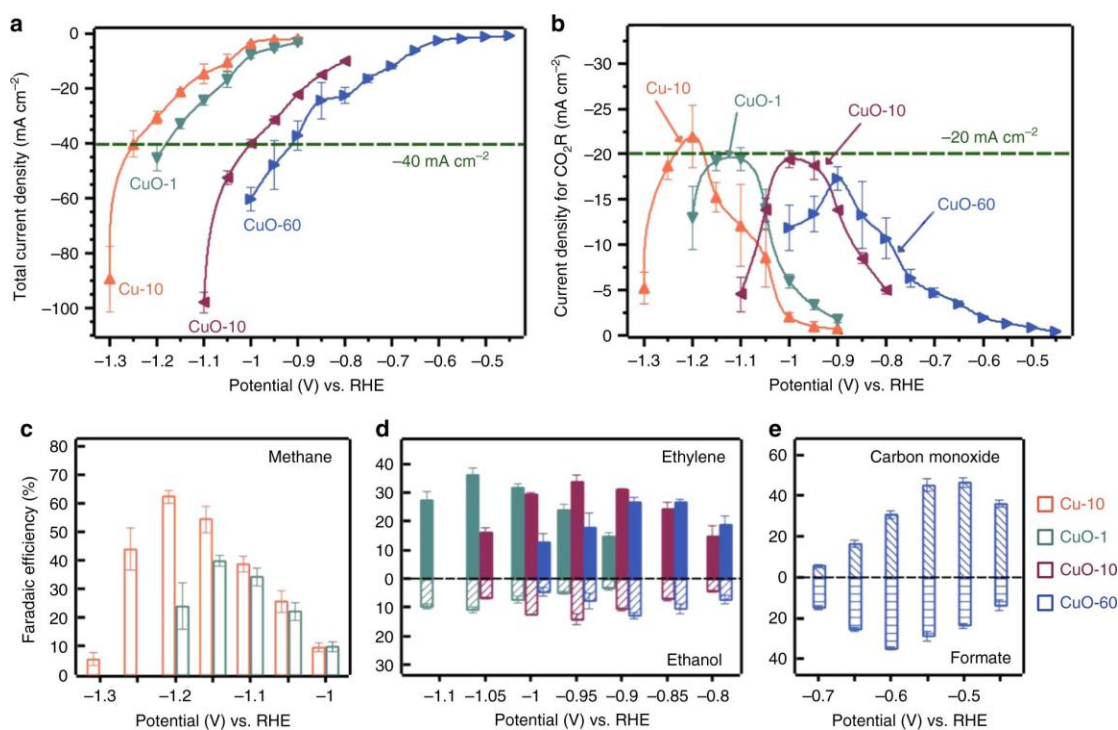
Figure 3.3. a) Total geometric current density; b) current density for CO_2 reduction; c) faradaic efficiency of methane on Cu-10 and CuO-1; d) faradaic efficiency of ethylene and ethanol on CuO-1, CuO-10, and CuO-60 catalysts; and e) faradaic efficiency of carbon monoxide and formate on CuO-60 catalyst [10].

3.1.2 The effects of catalyst structure

24

According to literature reports, noble metals and ionic liquids were competent to selectively reduce CO_2 to CO with high selectivity at low current density [13]. Unfortunately, they were restricted for bulk application due to high cost. Inspired by solid oxide fuel cell and hollow fiber from nickel and stainless steel, Recep Kas et al [14] prepared Cu hollow fibers used for CO production. The Cu hollow fibers could be employed as both gas diffuser and cathode attributed to a defect-rich porous structure as well as extraordinary improvement in mass transport (Figure 3.4). The hydrogen evolution was suppressed while the current density was unprecedentedly high at low potentials. Hence, CO_2 was converted with total faradaic efficiencies up to 85% at overpotentials between 200 and 400 mV, and 75% CO faradaic efficiency was achieved at a potential of -0.4 V versus RHE [15], which showed excellent performance compared with other catalysts (Figure 3.5).
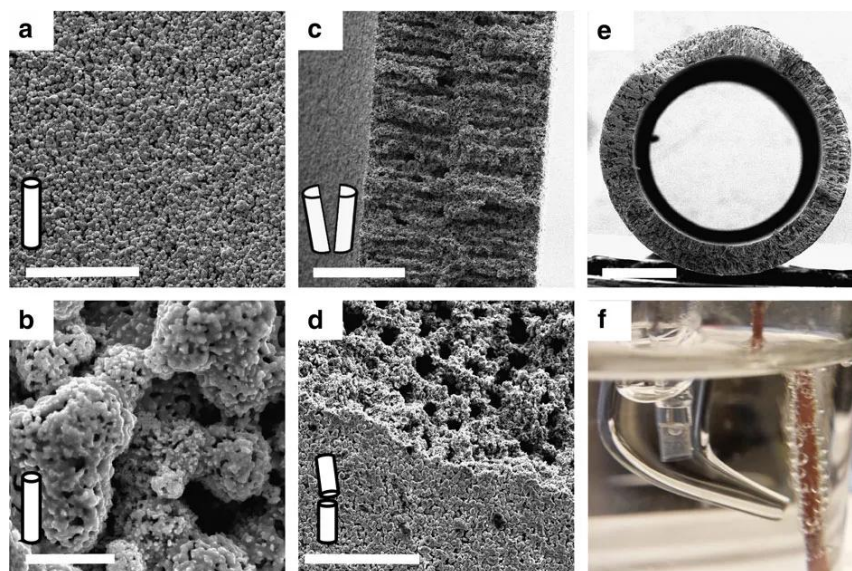
Figure 3.4. SEM images of Cu hollow fibers: a) outer surface, 50 mm; b) outer surface, 2 mm; c) cross-sectional of a perpendicularly broken, 100 mm; d) outer surface and cross-section in the parallel direction to the length, 50 mm, e) cross-sectional image of the Cu hollow fiber, 500 μm; and f) Cu hollow fiber employed as an electrode at 20 mL min^{-1} gas flow [14].
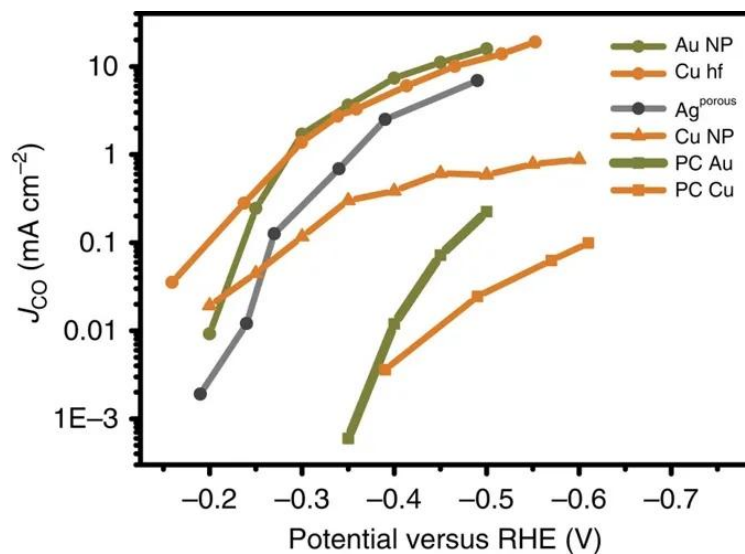
Figure 3.5. Comparison of the performance of different electrodes on the basis of the partial current density with CO at variable potentials [14].

3.1.3 The effects of pH value

The pH value at the electrode/electrolyte interface is proved to greatly influence the selectivity of final products. High pH is prone to CO coupling which further produces C_2H_4 [16]. In order to further improve the selectivity of hydrocarbon products affected by pH, Cu nanowire was synthesized with different length and density (longer length was corresponding with higher density). Longer Cu nanowire electrode was always surrounded with higher pH electrolyte, because the HCO_3^- in electrolyte was hard to diffuse into the Cu NW arrays and the OH^- generated by CO_2 reduction was hard to diffuse out the Cu NW arrays (Figure 3.6). C_2H_4 accompanied with other products (e.g C_2H_6 and ethanol) were generated on relatively longer Cu nanowires [17]. The result was supported by previous conclusion that CO coupling step was favored at a high local pH near the catalyst surface [18]. It could be an efficient approach to systematically control products on Cu nanowire by varying Cu nanowire length and even pH of electrolyte.
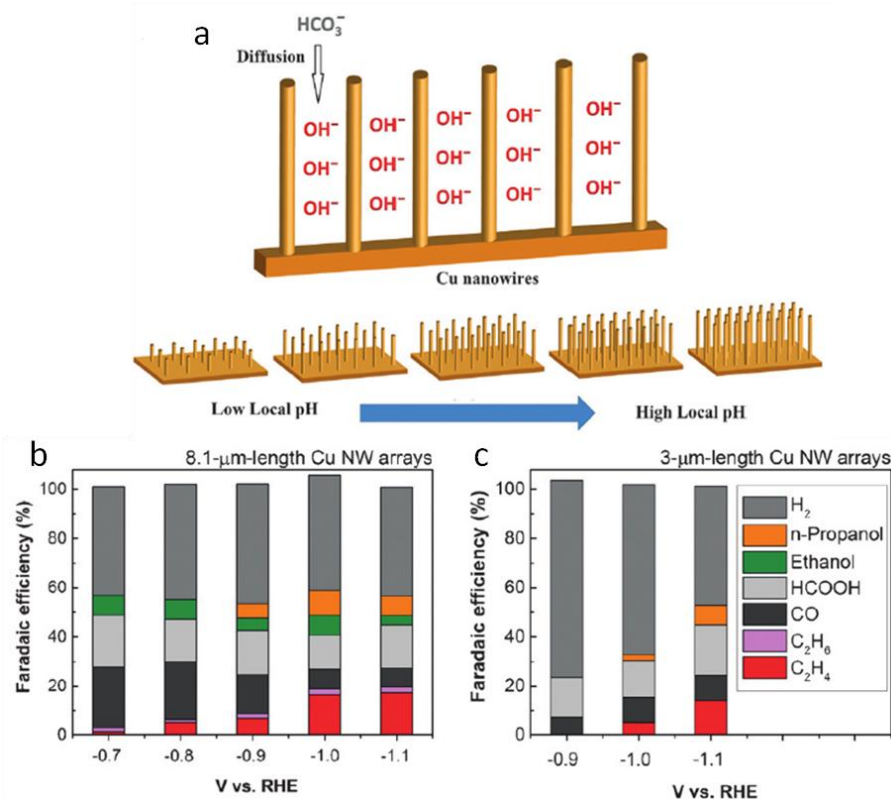
Figure 3.6. a) Schematic illustration of the diffusion of electrolytes into Cu nanowire arrays; b and c) faradaic efficiency of various products at 8.1- μm-length Cu NW arrays and 3- μm-length Cu NW arrays, respectively [17].

3.1.4 The effects of particle size

It is well known that varying the size of the catalytically active species is another strategy to tune surface chemisorption and enhance catalytic activities and selectivity in many reactions, such as ammonia synthesis, hydrogenation, electrocatalytic CO oxidation [19,20]. In 2014, Rulle Reske et al [21] investigated the size effects of Cu nanoparticles (NP) on the CO_2 reduction activity and, in particular, on product selectivity. The results showed the particles from 2 to 15 nm caused unexpected selectivity and activity variation. Generally, Cu NP exhibited higher current densities as the size decreased, which meant smaller size may cause higher activity, especially when the size was smaller than 5 nm (Fig 3.7). However, high activity was not

equivalent to high selectivity. If CO and H_2 were the preferred products to serve as feedstock for gas-to-liquid reaction technologies, the smaller size of Cu nanoparticles may be the better choice, while size smaller than 5 nm should be avoided for hydrocarbon products. Here, it was deduced that small Cu size may cause strong bonding between intermediate reaction species (*CO and *H) and catalyst, inhibiting the mobility of CO and H to form hydrocarbon.
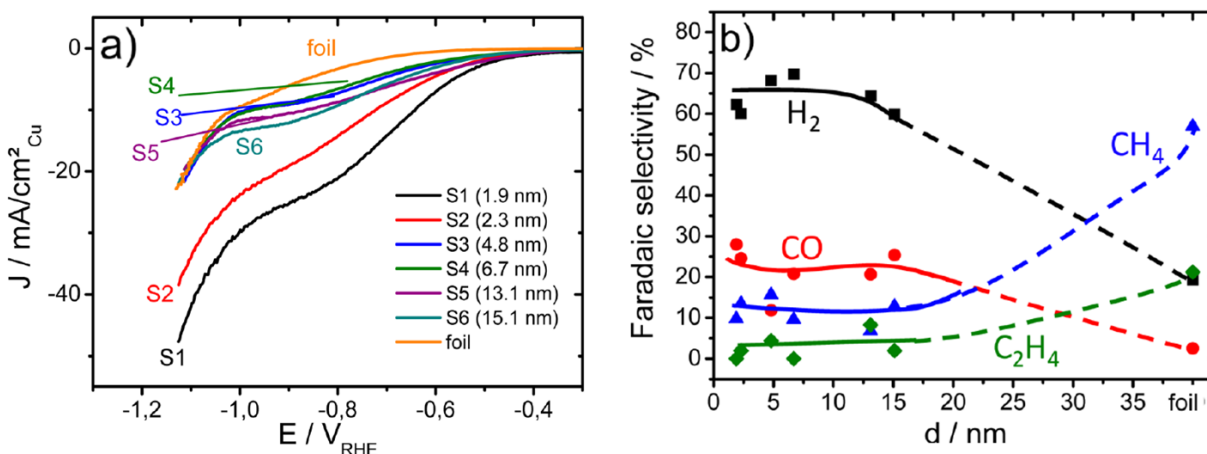
Figure 3.7. a) Linear sweep voltammetry and; b) composition of gaseous products of CO_2 reduction on Cu NP with different size [21].

3.1.5 The effects of subsurface oxygen

It has been reported by many groups that oxide-derived copper showed higher CO binding energy which changed the products of CO_2 reduction [22,23]. However, the mechanism of this phenomenon was not clear until Andre Eilert et al [24] proved the presence of oxygen and absence of oxide copper based on Ambient Pressure X-ray Photoelectron Spectroscopy (APXPS) and quasi in situ Electron Energy Loss Spectroscopy (EELS). In 2016, Andre Eilert et al exposed a polycrystalline copper to electrochemical oxidation-reduction cycles to prepare the catalyst. Results showed the new catalyst improved overall CO_2 reduction activity and product yield towards more ethylene versus methane (Fig3.8). It was proposed that residual subsurface oxygen

formed by oxidation-reduction cycles changed the electronic structure of the catalyst and created

sites with higher carbon monoxide binding energy by reducing the σ-repulsion. Therefore, C-C

bond formation was kinetically favored due to higher CO coverage on the catalyst [25,26].
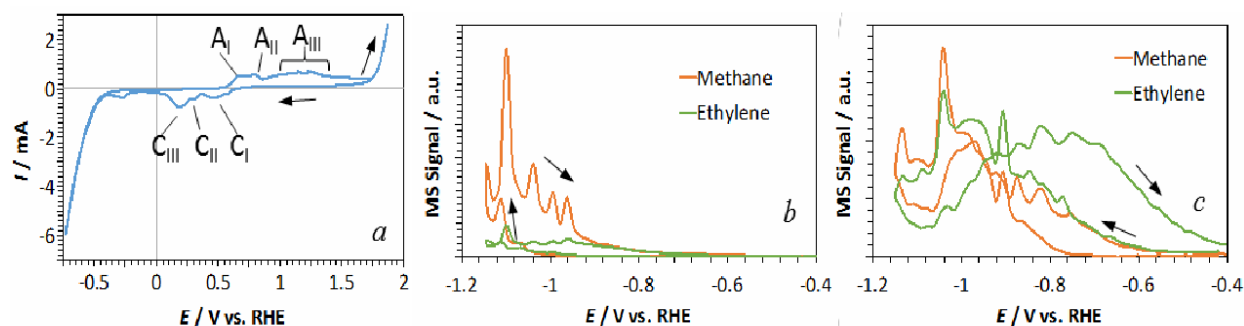
Figure 3.8. a) Cyclic voltammogram of an oxidation-reduction cycle of Cu in 0.1 M KHCO$_3$ and 4 mM KCl; b and c) online electrochemical mass spectrometry results of CO$_2$ reduction with polycrystalline Cu (b) and Cu after an oxidation-reduction cycle (c) [24].

3.1.6 The effects of sulfur and surface defect

Atomic vacancy defects influence electrocatalytic performance by adjusting the electronic

structure of neighboring atoms and consequently influence the energy barriers of the rate-

limiting reaction intermediates [27,28]. A core-shell nanoparticles structure catalyst designated

as Cu$_2$S-Cu-V (where V denotes vacancy) was synthesized based on the theory that copper

sulfide could provide a means to form stable surface defects and control the density of surface

vacancies by introducing sulfur into the Cu structure (Figure 3.9). Due to the synergetic effect of

Cu$_2$S core and the surface copper vacancies, the Cu$_2$S-Cu-V played an excellent role in

suppressing unwanted C$_2$ products and shifted product distribution towards alcohols [29].
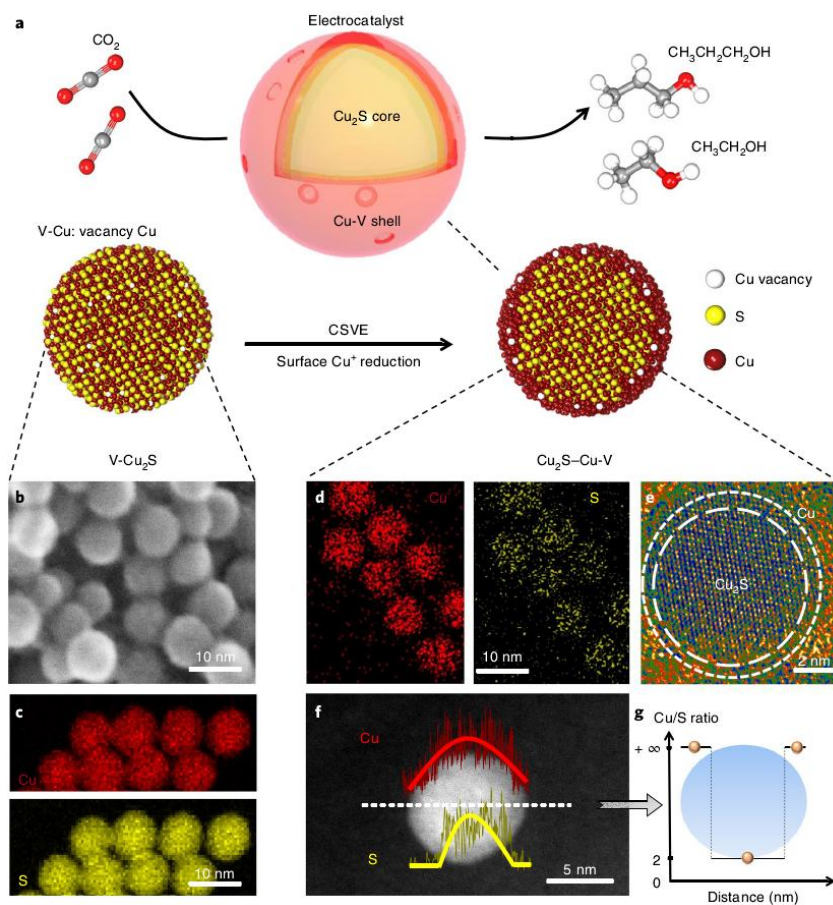
Figure 3.9. Catalyst design and structural characterization. a) Schematic illustration of Cu_2S-Cu-V electrocatalyst design; b) TEM and c) EDS mapping of the original V-Cu_2S nanoparticles; d) EDS mapping; e) high-resolution TEM; f) EDS line scan and g) the ratio of Cu/S concentration of the reduced Cu_2S-Cu-V nanocatalysts after electrochemical reduction. V-Cu indicates Cu with surface vacancies [29].

3.2 Cu alloy catalysts

Previous work has demonstrated that electrochemical CO_2 reduction with a planar Cu foil as the catalyst will produce at least 16 different products in varying quantities, which require high energy consumption in product separation. Cu-based bimetallic catalysts have been recognized as another class catalysts for CO_2 electroreduction at lower overpotential. It possesses the ability to produce specific products by modulating the adsorption and desorption of key intermediates on the catalyst surface. In the past years, many published research reported to focus on developing bimetallic Cu-based catalysts. Recent research indicated that different pattern and distribution of the bimetallic catalyst impacted not only product distribution, but also the yield [30].

3.2.1 The selectivity to CH$_4$

Copper based catalysts are well known for the conversion of CO_2 to CO and other deep reduction products with relatively favorable efficiencies at room temperature. In 2018, 4% Cu-doped CeO_2 nanorods electrocatalyst was used for CH_4 production with a faradaic efficiency as high as 58% at -1.8V [31]. In this type of catalyst, copper was well dispersedly loaded on the CeO_2 at the single atomic/ionic level preventing the copper being oxidized and aggregating. There were up to three oxygen vacancies around each Cu site because of the substitution action of Cu (Figure 3.10). The synergetic effect of Cu, CeO and oxygen vacancy resulted in a highly effective catalytic site for electroreduction. The result also mentioned that the C-C banding was substantially prohibited on the catalyst due to atomic dispersion of the electrocatalytic Cu sites, dramatically enhancing CH_4 formation [32,33].
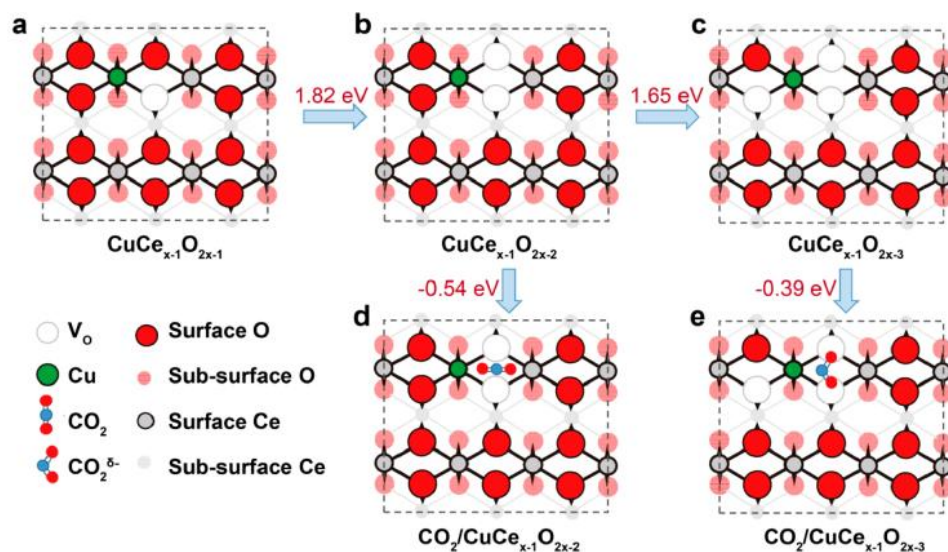
Figure 3.10. Theoretical calculations of the most stable structures of Cu-doped CeO_2 (110) and their effects on CO_2 activation [31].

3.2.2 The selectivity for syngas

Though Cu-based catalysts have excellent performance for CO_2 reduction, there are still two problems need to be solved, poor resistance to oxidation and selectivity. To solve the problems, an ultrathin $Cu/Ni(OH)_2$ nanosheets catalyst was engineered using sodium formate as protector to prevent Cu being oxidized and $Ni(OH)_2$ as supporter for preventing Cu nanosheets from being sintered during electrocatalysis (Figure 3.11A-E). Because the redox potential of $HCOO^-$ was lower than Cu, $HCOO^-$ suppressed oxidation of Cu similar to the cathodic protection in galvanized iron pipes. $Cu/Ni(OH)_2$ exhibited both excellent CO_2 adsorption ability and superior charge transport kinetics. It was cost-effective, and the nanosheets provided a current density of 4.3 mA cm^{-2} with a CO Faradaic efficiency of 92% at a low overpotential of -0.39 V. Interestingly, syngas was the only products and the ratio of CO and H_2 was tunable by applying different potentials [34,35]. The high selectivity may be attributed to the following reasons: 1) $Cu/Ni(OH)_2$ had excellent ability to absorb CO_2 while poor ability to absorb CO; 2) $Cu/Ni(OH)_2$

exhibited a superior charge transport kinetics; 3) the existence of $HCOO^-$ prevented the Cu from being oxidized; 4) the Cu was well dispersed (Figures 3.11 F, G).
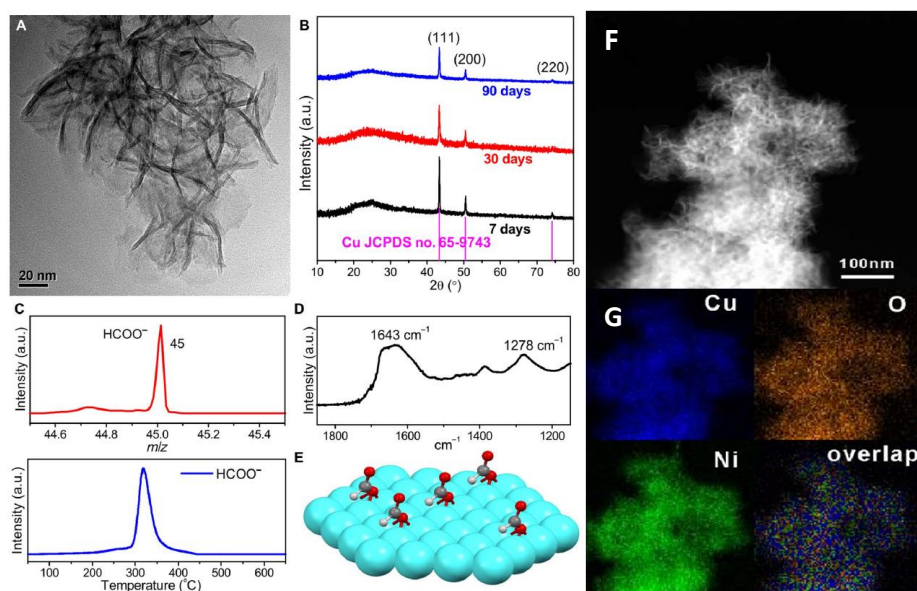
Figure 3.11. A) TEM image of the $Cu/Ni(OH)_2$ nanosheets after being stored in air at room temperature for 90 days; B) XRD patterns of the nanosheets after storing in air at room temperature for 7 to 90 days; c) TPD-MS profiles of the $Cu/Ni(OH)_2$ nanosheets heated in vacuum, whereas the bottom shows relative ionization intensities of the main decomposition products at different temperatures, the top displays the accumulative ionization intensity (m/z, mass/charge ratio); D) FTIR spectrum of the nanosheets and E) adsorption model of formate on Cu (color codes: cyan, Cu; red, O; gray, C; white, H). F) STEM and G) EDX mapping images of the $Cu/Ni(OH)_2$ nanosheets [34].

When particle size was between 5 and 15 nm, Cu exhibited similar catalytic selectivity in hydrocarbon formation, while the catalytic performance and selectivity unexpectedly increased with decreasing Cu particle size when its size was below 5 nm. Meanwhile, previous work proved that finely controlled size of Pd displayed high Faradaic efficiency and current density for CO production. Here, Zhen Yin et al [36] synthesized the Cu-Pd bimetallic alloy with different ratio supported on carbon to produce CO. $Pd_{85}Cu_{15}/C$ catalyst showed good activity and

selectivity (Figure 3.12) because the rate-determining steps of CO_2 absorption and CO desorption were improved while the H^+ combination was inhibited due to synergistic effect of electronic effect and geometric effect.
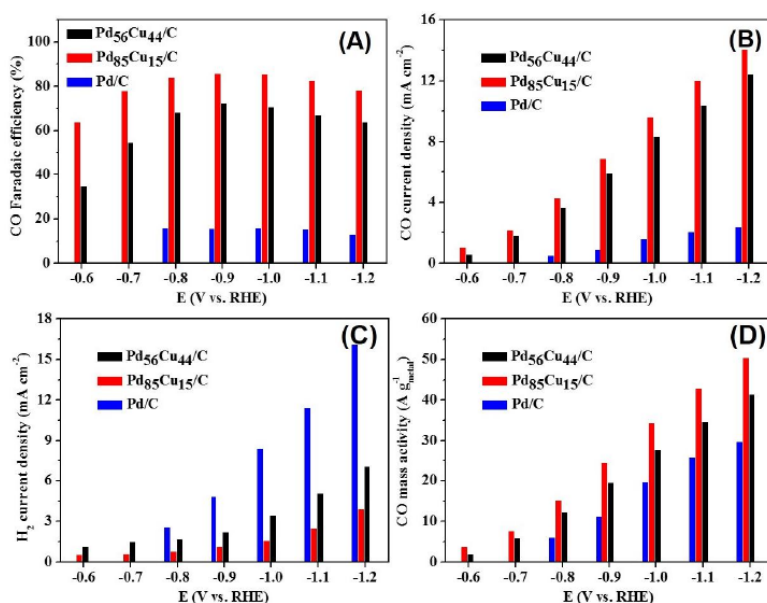
Figure 3.12. CO_2 reduction activity over PdCu/C and Pd/C catalysts in CO_2-saturated 0.1 M $KHCO_3$ solution [36].

3.2.3 The selectivity for multiple-carbon products

Recently, many alloying catalysts have been synthesized to convert CO_2 to multiple-carbon products, especially oxygenated species such as alcohols, because these products are generally more valuable than their hydrocarbon counterparts and they are in liquid form under ambient conditions which simplify the subsequent processing, storage, and distribution [37].

CuPd nanoalloys

It was another challenge to evaluate the relationship between the atomic arrangements/ ratios (Figure 3.13) and the performance of CO_2 reduction. Related studies [38] were conducted to elucidate the mechanism, showing the phase-separated bimetallic catalysts produced C_2

chemicals while the well-ordered catalysts favored the conversion of CO_2 to CH_4. For the phase-separated catalysts, the Cu atoms structure may allow for favorable molecular distance and small steric hindrance for dimerizing *CO and *COH which were further converted to C_2 products. While for the ordered structure, Pd stabilized surface *CHO which were further converted to CH_4. It was shown that electronic effect played less important role than geometric/structural effect which determined catalytic selectivity and activity, because Cu had much higher d-band position than PdCu. It was further proved that Cu had much better performance to produce C_2 than that of Pd (Figure 3.14). Based on a literature report, the orientation of intermediate toward the active sites influenced the reaction, similarly, different ratios of component in the bimetallic catalysts caused various orientations of the intermediate on the surface, therefore led to different selectivity [39].
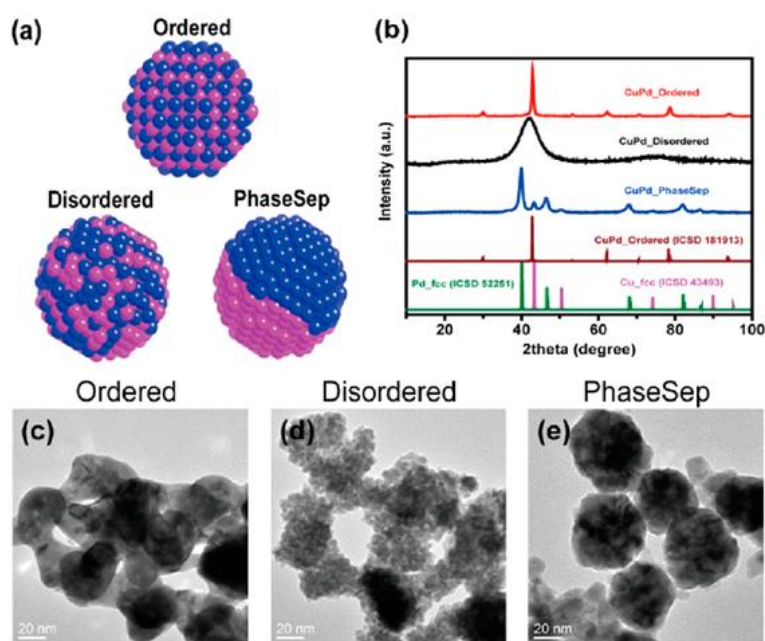
Figure 3.13. a) Illustration of the prepared CuPd nanoalloys with different structures; b) XRD patterns of CuPd nanoalloys, Cu, Pd and CuPd alloys; c-e) high-resolution TEM images of Cu (red) and Pd (green) [38].
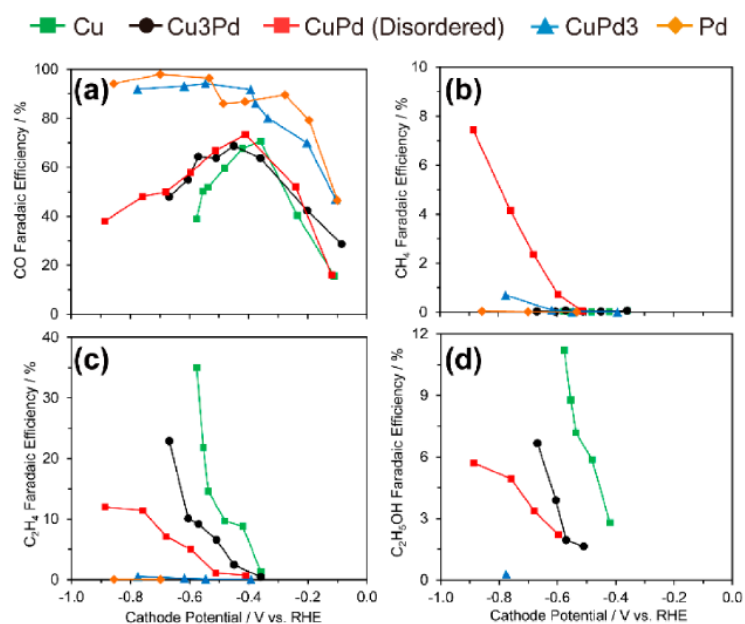
Figure 3.14. Faradaic efficiencies for a) CO; b) CH_4; c) C_2H_4; d) C_2H_5OH for catalysts with different Cu:Pd ratios: Cu, Cu_3Pd, CuPd, $CuPd_3$, and Pd [38].

CuZn nanoalloys

Among all products from the reduction of CO_2, ethanol is an attractive liquid fuel. However, due to the barrier of higher energy needed for C-C coupling, previously mentioned Cu nanostructure only produced ethanol with faradaic efficiency generally < 20 % while ethylene as the primary C_2 product [40]. Though heteroatoms have been added to Cu to improve selectivity between ethanol and ethylene, it is hard to realize both high partial current and high selectivity [41]. In order to overcome the shortcoming, ZnO was used to modify the CuO nanowires surface using atomic layer deposition (ALD) to improve selectivity. Compared to commonly used methods, such as electrodeposition, annealing or solution processing, ALD was flexible to adjust various bimetallic structures and/or the ratio between different metallic components. As a result, 48.6 % faradaic efficiency and 97 mA cm^{-2} partial current density for C_2 liquids was achieved at -0.68 V. 32 % faradaic efficiency of ethanol was formed at -1.15 V and the partial current density increased from 7.5 mA cm^{-2} on Cu to 10.5 mA cm^{-2} on CuZn. According to the

37

systematic analysis of the electrocatalytic behavior, it was believed that the presence of Zn modified the binding energy of CO on Cu, which was combined with $*CH_3$ to form $*COCH_3$, a precursor of ethanol [42].

Scientists also propose to alloy Ag with Cu to bring their superiority into full play, because Ag is a highly selective catalyst for CO production while Cu possesses the capability to further reduce CO to more valued products [43,44]. CuAg nanoporous structure catalyst was synthesized using 3,5-diamino-1,2,4-triazole (DAT) as an inhibitor (Figure 3.15). Because of the existence of DAT, the nucleation of Cu or Ag was inhibited, and Cu and Ag were homogeneously mixed via electrodeposition. The catalyst exhibited excellent efficiency with about 60% C_2H_4 and 25% C_2H_5OH at a relatively low applied potential (-0.7 V vs. RHE) and a high current density (300 mA cm^{-2}) [45]. According to previous research results [46], Cu_2O was mainly responsible for high yield of CH_3OH. It was deduced here that high selectivity towards C_2H_4 and C_2H_5OH was because the incorporation of Ag into the alloy. In one aspect, Ag oxide could be reduced by Cu due to the formation enthalpies of Cu_2O (-169 kJ mol^{-1}) and Ag_2O (-31.1 kJ mol^{-1}); In another aspect, Cu was more likely to be oxygenated to Cu_2O because Cu atoms in the CuAg samples tended to carry a slightly positive charge. In 2018, Drew Higgins [47] prepared CuAg thin films with nonequilibrium Cu/Ag alloying for CO_2 reduction, further explaining why Ag could improve the selectivity to C_2 products. The results indicated that though the overall reduction activity decreased for CuAg versus Cu, Ag miscibility into Cu increased the activity and selectivity toward liquid carbonyl products likely due to the decreased surface binding energies of oxygen-containing intermediate species. Meanwhile, it was observed that the competing products of hydrocarbons and H_2 were significantly suppressed. Density functional theory (DFT) simulation suggested that Ag doped in Cu weakened the binding energy of $*H$ species, causing

the steadily decrease in activity and selectivity toward hydrocarbons and the H_2 when the ratio of Ag/Cu increased. The better understanding of the underlying mechanisms may further improve selectivity toward liquid carbonyl products.
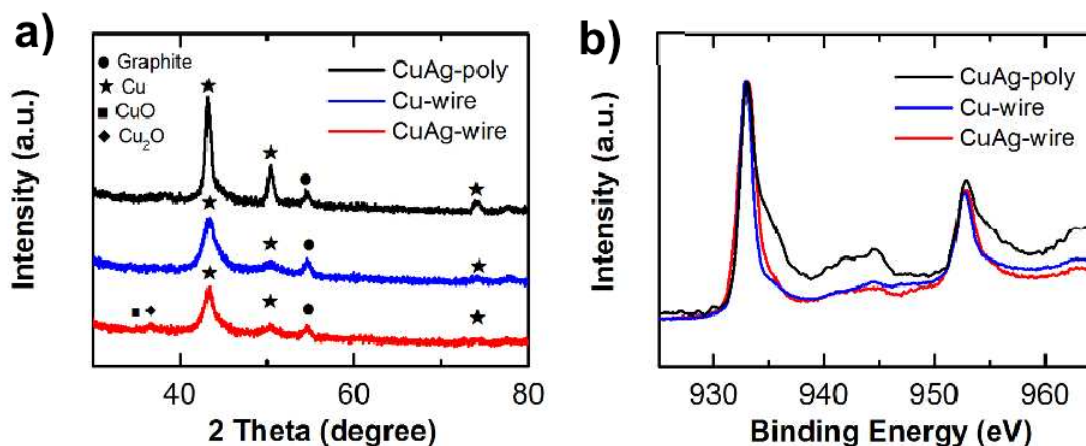
Figure 3.15. a) XRD and b) XPS patterns of CuAg-poly (6% Ag) electrodeposited without DAT, Cu-wire (0% Ag) electrodeposited with DAT, and CuAg-wire (6% Ag) electrodeposited with DAT [45].

3.3 Organic Cu

It was reported that the hydrophobicity of electrode was regarded as an determinant on the selectivity of CO_2 reduction, because its submerged hydrophobic surfaces trapped appreciable amounts of gas at the nanoscale which facilitates CO_2 accumulation at the Cu-solution interface [48,49]. Inspired by the plastrons of diving bell spider composed of hydrophobic hairs that trapped air and thereby allowed the spider to respire under water, a hierarchically structured Cu dendrites electrode was synthesized with super hydrophobic surface generated by 1-octadecanethiol treatment (Figure 3.16). As a result, H_2 evolution was substantially suppressed from 71% faradaic efficiency to 10%, while CO_2 reduction was increased from 24% to 86%, of which C_2 products comprised 74% FE [50].
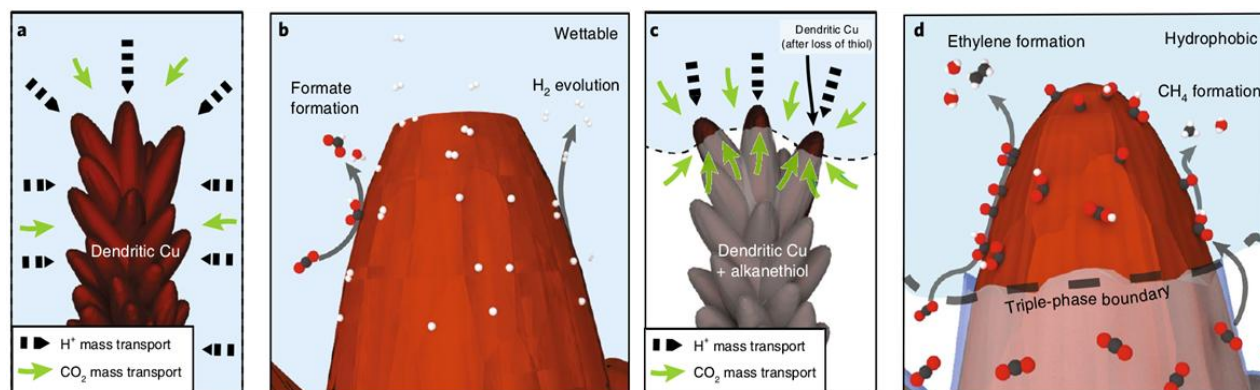
Figure 3.16. The illustration of a-b) wettable dendrite electrode and c-d) hydrophobic dendrite electrode for electroreduction [50].

Zhe Weng et al [51] synthesized a Cu centered organic catalyst in 2016, copper-porphyrin complex (copper(II)-5,10,15,20-tetrakis-(2,6-dihydroxyphenyl) porphyrin), called PorCu (Figure 3.17). It was used as a heterogeneous electrocatalyst for reducing CO_2 to hydrocarbons in aqueous media. At the point of -0.976 V, the partial current densities of CH_4 and C_2H_4 were 13.2 and 8.4 mA cm^{-2}, while the corresponding turnover frequencies were 4.3 and 1.8 molecules $site^{-1}$ s^{-1}, respectively. The catalytic reaction rates for hydrocarbon products were higher than other reported molecular metal complex catalyst and most Cu based electrocatalysts at around ~-1 V. It was considered the Cu center and OH groups in the porphyrin structure played indispensable role for the high conversion [52,53]. Especially, the PorCu molecular structure with the Cu center in the +1 oxidation state worked as the active catalyst for electrochemically converting CO_2 to CH_4 and C_2H_4, and the OH groups may help bind certain reaction intermediates or provide an intra molecular source of protons.
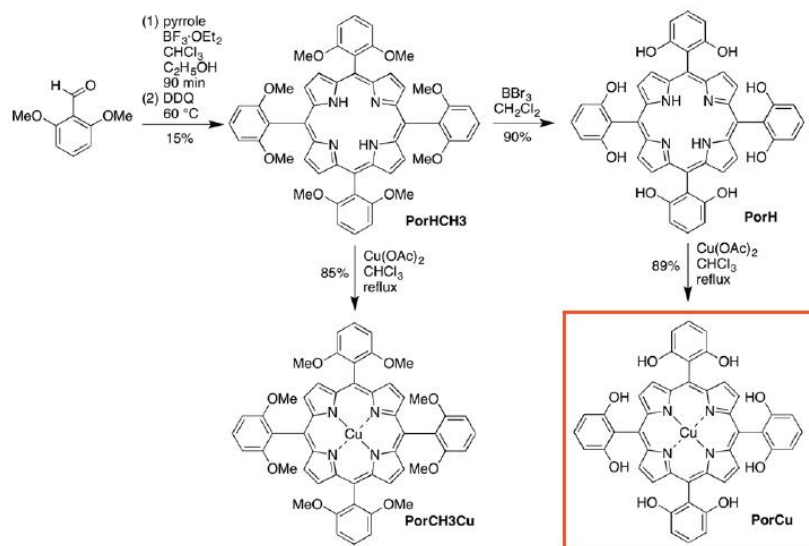
Figure 3.17. Synthetic routes for copper-porphyrin molecular catalysts [51].

3.4 Conclusion

In this chapter, we discuss why Cu is the most popular metal and briefly introduce the electrochemical cell used for CO_2 electroreduction. Furthermore, referring to recent representative Cu-based catalysts, we illustrate factors influencing the performance of catalysts and primarily explain how those factors impact the activity and selectivity of CO_2 conversion. Those factors are pH value, morphology, particle sizes, the presence of atomic-scale defects, surface roughness, and/or residual oxygen atoms, and so on. In summary, these factors can benefit selectivity and yield by optimizing binding capability of CO_2 and intermediates, suppressing hydrogen formation and improving electron transportation. There are many methods that are introduced to optimize the performance of Cu-based catalyst. For example, doping Cu with other metal proves to be an effective and feasible option. Doping may help change both the inner structure and outer structure simultaneously, further optimizing the binding energy, improving electron transportation and suppressing hydrogen formation. This chapter can guide us to produce more ideal catalysts, in addition, the information presented in this chapter can be a foundation to summarize the property and mechanism in next chapter.

Nevertheless, it is very difficult to fairly and objectively compare current results used for analyzing the catalytic performance of different catalysts due to a lack of standardized methods for measuring and reporting activity data [54]. The conversion rate of CO_2 is influenced by catalyst type, electrolyte, hydrodynamics of the electrochemical cell, etc. Hence, the recommended measurements should evaluate the data in the absence of a convolution of intrinsic kinetics and mass transport effects and will not introduce artifacts from impurities, either from the electrolyte or counter electrode. In addition, electrochemical reactions rates should be

normalized to both the geometric electrode area and the electrochemically active surface area to facilitate the comparison of reported catalysts [55,56].

Reference

[1] Zhao, C., & Wang, J. (2016). Electrochemical reduction of CO_2 to formate in aqueous solution using electro-deposited Sn catalysts. Chemical Engineering Journal, 293, 161-170.

[2] Wu, J., Risalvato, F. G., Ma, S., & Zhou, X. D. (2014). Electrochemical reduction of carbon dioxide III. The role of oxide layer thickness on the performance of Sn electrode in a full electrochemical cell. Journal of Materials Chemistry A, 2(6), 1647-1651.

[3] Bagger, A., Ju, W., Varela, A. S., Strasser, P., & Rossmeisl, J. (2017). Electrochemical CO_2 reduction: a classification problem. ChemPhysChem, 18(22), 3266-3273.

[4] Hori, Y., Wakebe, H., Tsukamoto, T., & Koga, O. (1994). Electrocatalytic process of CO selectivity in electrochemical reduction of CO_2 at metal electrodes in aqueous media. Electrochimica Acta, 39(11-12), 1833-1839.

[5] Kuhl, K. P., Cave, E. R., Abram, D. N., & Jaramillo, T. F. (2012). New insights into the electrochemical reduction of carbon dioxide on metallic copper surfaces. Energy & Environmental Science, 5(5), 7050-7059.

[6] De Luna, P., Quintero-Bermudez, R., Dinh, C. T., Ross, M. B., Bushuyev, O. S., Todorović, P., ... & Sargent, E. H. (2018). Catalyst electro-redeposition controls morphology and oxidation state for selective carbon dioxide reduction. Nature Catalysis, 1(2), 103-110.

[7] Reske, R., Mistry, H., Behafarid, F., Roldan Cuenya, B., & Strasser, P. (2014). Particle size effects in the catalytic electroreduction of CO_2 on Cu nanoparticles. Journal of the American Chemical Society, 136(19), 6978-6986.

[8] Li, C. W., Ciston, J., & Kanan, M. W. (2014). Electroreduction of carbon monoxide to liquid fuel on oxide-derived nanocrystalline copper. Nature, 508(7497), 504.

[9] Handoko, A. D., Ong, C. W., Huang, Y., Lee, Z. G., Lin, L., Panetti, G. B., & Yeo, B. S. (2016). Mechanistic insights into the selective electroreduction of carbon dioxide to ethylene on Cu_2O-derived copper catalysts. The Journal of Physical Chemistry C, 120(36), 20058-20067.

[10] Ren, D., Fong, J., & Yeo, B. S. (2018). The effects of currents and potentials on the selectivities of copper toward carbon dioxide electroreduction. Nature communications, 9(1), 925.

[11] Singh, M. R., Kwon, Y., Lum, Y., Ager III, J. W., & Bell, A. T. (2016). Hydrolysis of electrolyte cations enhances the electrochemical reduction of CO_2 over Ag and Cu. Journal of the American Chemical Society, 138(39), 13006-13012.

[12] Lum, Y., Yue, B., Lobaccaro, P., Bell, A. T., & Ager, J. W. (2017). Optimizing C-C coupling on oxide-derived copper catalysts for electrochemical CO_2 reduction. The Journal of Physical Chemistry C, 121(26), 14191-14203.

[13] Lu, Q., Rosen, J., Zhou, Y., Hutchings, G. S., Kimmel, Y. C., Chen, J. G., & Jiao, F. (2014). A selective and efficient electrocatalyst for carbon dioxide reduction. Nature communications, 5, 3242.

[14] Kas, R., Hummadi, K. K., Kortlever, R., De Wit, P., Milbrat, A., Luiten-Olieman, M. W., ... & Mul, G. (2016). Three-dimensional porous hollow fibre copper electrodes for efficient and high-rate electrochemical carbon dioxide reduction. Nature communications, 7, 10748.

[15] Ma, M., Trześniewski, B. J., Xie, J., & Smith, W. A. (2016). Selective and efficient reduction of carbon dioxide to carbon monoxide on oxide-derived nanostructured silver electrocatalysts. Angewandte Chemie, 128(33), 9900-9904.

[16] Schouten, K. J. P., Qin, Z., Pérez Gallent, E., & Koper, M. T. (2012). Two pathways for the formation of ethylene in CO reduction on single-crystal copper electrodes. Journal of the American Chemical Society, 134(24), 9864-9867.

[17] Ma, M., Djanashvili, K., & Smith, W. A. (2016). Controllable hydrocarbon formation from the electrochemical reduction of CO_2 over Cu nanowire arrays. Angewandte Chemie International Edition, 55(23), 6680-6684.

[18] Kas, R., Kortlever, R., Yılmaz, H., Koper, M. T., & Mul, G. (2015). Manipulating the hydrocarbon selectivity of copper nanoparticles in CO_2 electroreduction by process conditions. ChemElectroChem, 2(3), 354-358.

[19] Gasteiger, H. A., Kocha, S. S., Sompalli, B., & Wagner, F. T. (2005). Activity benchmarks and requirements for Pt, Pt-alloy, and non-Pt oxygen reduction catalysts for PEMFCs. Applied Catalysis B: Environmental, 56(1-2), 9-35.

[20] Merte, L. R., Behafarid, F., Miller, D. J., Friebel, D., Cho, S., Mbuga, F., ... & Nilsson, A. (2012). Electrochemical oxidation of size-selected Pt nanoparticles studied using in situ high-energy-resolution X-ray absorption spectroscopy. ACS Catalysis, 2(11), 2371-2376.

[21] Reske, R., Mistry, H., Behafarid, F., Roldan Cuenya, B., & Strasser, P. (2014). Particle size effects in the catalytic electroreduction of CO_2 on Cu nanoparticles. Journal of the American Chemical Society, 136(19), 6978-6986.

[22] Lee, S., Kim, D., & Lee, J. (2015). Electrocatalytic production of C3-C4 compounds by conversion of CO_2 on a chloride-induced bi-phasic Cu_2O-Cu catalyst. Angewandte Chemie International Edition, 54(49), 14701-14705.

[23] Kuhl, K. P., Hatsukade, T., Cave, E. R., Abram, D. N., Kibsgaard, J., & Jaramillo, T. F. (2014). Electrocatalytic conversion of carbon dioxide to methane and methanol on transition metal surfaces. Journal of the American Chemical Society, 136(40), 14107-14113.

[24] Eilert, A., Cavalca, F., Roberts, F. S., Osterwalder, J., Liu, C., Favaro, M., ... & Nilsson, A. (2016). Subsurface oxygen in oxide-derived copper electrocatalysts for carbon dioxide reduction. The journal of physical chemistry letters, 8(1), 285-290.

[25] Liu, C., Lourenço, M. P., Hedström, S., Cavalca, F., Diaz-Morales, O., Duarte, H. A., ... & Pettersson, L. G. (2017). Stability and effects of subsurface oxygen in oxide-derived Cu catalyst for CO_2 reduction. The Journal of Physical Chemistry C, 121(45), 25010-25017.

[26] Cavalca, F., Ferragut, R., Aghion, S., Eilert, A., Diaz-Morales, O., Liu, C., ... & Nilsson, A. (2017). Nature and distribution of stable subsurface oxygen in copper electrodes during electrochemical CO_2 reduction. The Journal of Physical Chemistry C, 121(45), 25003-25009.

[27] Liu, X., Wang, X., Zhou, B., Law, W. C., Cartwright, A. N., & Swihart, M. T. (2013). Size-controlled synthesis of $Cu_{2-x}E$ (E = S, Se) nanocrystals with strong tunable near-infrared localized surface plasmon resonance and high conductivity in thin films. Advanced Functional Materials, 23(10), 1256-1264.

[28] Luther, J. M., Jain, P. K., Ewers, T., & Alivisatos, A. P. (2011). Localized surface plasmon resonances arising from free carriers in doped quantum dots. Nature materials, 10(5), 361.

[29] Zhuang, T. T., Liang, Z. Q., Seifitokaldani, A., Li, Y., De Luna, P., Burdyny, T., ... & Dinh, C. T. (2018). Steering post-C–C coupling selectivity enables high efficiency electroreduction of carbon dioxide to multi-carbon alcohols. Nature Catalysis, 1(6), 421.

[30] Peterson, A. A., & Nørskov, J. K. (2012). Activity descriptors for CO_2 electroreduction to methane on transition-metal catalysts. The Journal of Physical Chemistry Letters, 3(2), 251-258.

[31] Wang, Y., Chen, Z., Han, P., Du, Y., Gu, Z., Xu, X., & Zheng, G. (2018). Single-atomic Cu with multiple oxygen vacancies on ceria for electrocatalytic CO_2 reduction to CH_4. ACS Catalysis, 8(8), 7113-7119.

[32] Manthiram, K., Beberwyck, B. J., & Alivisatos, A. P. (2014). Enhanced electrochemical methanation of carbon dioxide with a dispersible nanoscale copper catalyst. Journal of the American Chemical Society, 136(38), 13319-13325.

[33] Li, Y., Cui, F., Ross, M. B., Kim, D., Sun, Y., & Yang, P. (2017). Structure-sensitive CO_2 electroreduction to hydrocarbons on ultrathin 5-fold twinned copper nanowires. Nano letters, 17(2), 1312-1317.

[34]Dai, L., Qin, Q., Wang, P., Zhao, X., Hu, C., Liu, P., ... & Mo, S. (2017). Ultrastable atomic copper nanosheets for selective electrochemical reduction of carbon dioxide. Science advances, 3(9), e1701069.

[35] Jin, M., He, G., Zhang, H., Zeng, J., Xie, Z., & Xia, Y. (2011). Shape-controlled synthesis of copper nanocrystals in an aqueous solution with glucose as a reducing agent and hexadecylamine as a capping agent. Angewandte Chemie International Edition, 50(45), 10560-10564.

[36] Yin, Z., Gao, D., Yao, S., Zhao, B., Cai, F., Lin, L., ... & Bao, X. (2016). Highly selective palladium-copper bimetallic electrocatalysts for the electrochemical reduction of CO_2 to CO. Nano Energy, 27, 35-43.

[37] Shaner, M. R., Atwater, H. A., Lewis, N. S., & McFarland, E. W. (2016). A comparative technoeconomic analysis of renewable hydrogen production using solar energy. Energy & Environmental Science, 9(7), 2354-2371.

[38] Ma, S., Sadakiyo, M., Heima, M., Luo, R., Haasch, R. T., Gold, J. I., ... & Kenis, P. J. (2016). Electroreduction of carbon dioxide to hydrocarbons using bimetallic Cu-Pd catalysts with different mixing patterns. Journal of the American Chemical Society, 139(1), 47-50.

[39] Schouten, K. J. P., Kwon, Y., Van der Ham, C. J. M., Qin, Z., & Koper, M. T. M. (2011). A new mechanism for the selectivity to C_1 and C_2 species in the electrochemical reduction of carbon dioxide on copper electrodes. Chemical Science, 2(10), 1902-1909.

[40] Pander III, J. E., Ren, D., Huang, Y., Loo, N. W. X., Hong, S. H. L., & Yeo, B. S. (2018). Understanding the Heterogeneous Electrocatalytic Reduction of Carbon Dioxide on Oxide-Derived Catalysts. ChemElectroChem, 5(2), 219-237.

[41] Lee, S., Park, G., & Lee, J. (2017). Importance of Ag-Cu biphasic boundaries for selective electrochemical reduction of CO_2 to ethanol. ACS Catalysis, 7(12), 8594-8604.

[42] Ren, D., Gao, J., Pan, L., Wang, Z., Luo, J., Zakeeruddin, S. M., ... & Grätzel, M. (2019). Atomic Layer Deposition of ZnO on CuO Enables Selective and Efficient Electroreduction of Carbon Dioxide to Liquid Fuels. Angewandte Chemie International Edition, 58(42), 15036-15040.

[43] Hatsukade, T., Kuhl, K. P., Cave, E. R., Abram, D. N., & Jaramillo, T. F. (2014). Insights into the electrocatalytic reduction of CO_2 on metallic silver surfaces. Physical Chemistry Chemical Physics, 16(27), 13814-13819.

[44] Hatsukade, T., Kuhl, K. P., Cave, E. R., Abram, D. N., Feaster, J. T., Jongerius, A. L., ... & Jaramillo, T. F. (2017). Carbon Dioxide Electroreduction using a Silver-Zinc Alloy. Energy Technology, 5(6), 955-961.

[45] Hoang, T. T., Verma, S., Ma, S., Fister, T. T., Timoshenko, J., Frenkel, A. I., ... & Gewirth, A. A. (2018). Nanoporous copper–silver alloys by additive-controlled electrodeposition for the selective electroreduction of CO_2 to ethylene and ethanol. Journal of the American Chemical Society, 140(17), 5791-5797.

[46] Le, M., Ren, M., Zhang, Z., Sprunger, P. T., Kurtz, R. L., & Flake, J. C. (2011). Electrochemical reduction of CO_2 to CH_3OH at copper oxide surfaces. Journal of the Electrochemical Society, 158(5), E45-E49.

[47] Higgins, D., Landers, A. T., Ji, Y., Nitopi, S., Morales-Guio, C. G., Wang, L., ... & Jaramillo, T. F. (2018). Guiding electrochemical carbon dioxide reduction toward carbonyls using copper silver thin films with interphase miscibility. ACS Energy Letters, 3(12), 2947-2955.

[48] Melnichenko, Y. B., Lavrik, N. V., Popov, E., Bahadur, J., He, L., Kravchenko, I. I., ... & Szekely, N. K. (2014). Cavitation on deterministically nanostructured surfaces in contact with an aqueous phase: A small-angle neutron scattering study. Langmuir, 30(33), 9985-9990.

[49] Raciti, D., & Wang, C. (2018). Recent advances in CO_2 reduction electrocatalysis on copper. ACS Energy Letters, 3(7), 1545-1556.

[50] Wakerley, D., Lamaison, S., Ozanam, F., Menguy, N., Mercier, D., Marcus, P., ... & Mougel, V. (2019). Bio-inspired hydrophobicity promotes CO_2 reduction on a Cu surface. Nature materials, 1-6.

[51] Weng, Z., Jiang, J., Wu, Y., Wu, Z., Guo, X., Materna, K. L., ... & Wang, H. (2016). Electrochemical CO_2 reduction to hydrocarbons on a heterogeneous molecular Cu catalyst in aqueous solution. Journal of the American Chemical Society, 138(26), 8076-8079.

[52] Savéant, J. M. (2008). Molecular catalysis of electrochemical reactions. Mechanistic aspects. Chemical Reviews, 108(7), 2348-2378.

[53] Lin, S., Diercks, C. S., Zhang, Y. B., Kornienko, N., Nichols, E. M., Zhao, Y., ... & Chang, C. J. (2015). Covalent organic frameworks comprising cobalt porphyrins for catalytic CO_2 reduction in water. Science, 349(6253), 1208-1213.

[54] Voiry, D., Chhowalla, M., Gogotsi, Y., Kotov, N. A., Li, Y., Penner, R. M., ... & Weiss, P. S. (2018). Best practices for reporting electrocatalytic performance of nanomaterials.

[55] Clark, E. L., Resasco, J., Landers, A., Lin, J., Chung, L. T., Walton, A., ... & Bell, A. T. (2018). Standards and protocols for data acquisition and reporting for studies of the electrochemical reduction of carbon dioxide. ACS Catalysis, 8(7), 6560-6570.

[56] Buriak, J. M., Jones, C. W., Kamat, P. V., Schanze, K. S., Schatz, G. C., Scholes, G. D., & Weiss, P. S. (2016). Virtual Issue on Best Practices for Reporting the Properties of Materials and Devices: Record Well, Repeat Often, Report Correctly.

Chapter 4 Performance and mechanism of Cu-based catalysts

Introduction

Electrochemistry has been becoming more and more important because of renewable energy consumption and storage. Progresses in controllable synthesis approaches and characterization of catalyst have significant benefit in understanding fundamental mechanism and developing highly efficient catalysts. Meanwhile, numerical models have being supplemented the experimental results to simulate the reaction path and calculate the energy cost. In this chapter, we will summarize and discuss the catalytic property and mechanism.

4.1 Catalytic performance

Cu-based catalysts are the most promising to realize commercial utilization for valued chemicals production, such as methane, ethanol and ethylene. Various types of Cu-based catalysts (pure Cu, Cu bimetallic, organic Cu, etc.) have been developed to achieve this goal [1]. Table 4.1 summarizes the cu-based catalysts and their performance for different chemical products in recent years.

Table 4.1. Summary of electrocatalytic reduction toward carbon products performance on different catalysts [1].

Catalyst	E/V	Faradaic efficiency/%						J_{C2+} (mA cm^{-2})
		CO	CH$_4$	C$_2$H$_4$	C$_2$H$_5$OH	propanol	C$_{2+}$	
Phase-separated CuPd [a]	-0.74			48	15			
Cu NCs/Cu foils [a]	-0.96			32			60.5	41
Ag-Cu core-shell [b]	-1.06		18	25				
Cu$_2$O derived Cu NP [b]	-1.1			19				
Cu mesocrystal [b]	-0.99		1.47	27.2				
Cu nanowire array [b]	-1.1			17.4		8		
Prism Cu [b]	-1.1						35	10
Cu NPs covered Cu foil [b]	-1.1		1				36	N.A.
Electropolished Cu foil [b]	-1.05						40.6	2.8
44-nm Cu cubic NPs [b]	-1.1			41			46.4	1.4
Cu NPs ensembles [b]	-0.75						～50	
3.6-um Cu$_2$O film [b]	-0.99			34.26	16.37		50.8	17.8
OD-Cu$_4$Zn [b]	-1.05						51	15
Cu$_{28}$Ag$_{72}$ [b]	Pulse			12.8	17.3		54.2	
Cu(100) single electrode [b]	-1		30.4	40.4	9.7	1.5	57.8	2.9
18-nm Cu [b]	-1.03			42.6	11.8	5.4	59.8	18.7
Cu(100) [b]	-0.97						60	2
Pd$_{85}$Cu$_{15}$/C [b]	-0.89	86						
Plasma Oxidized Cu [b]	-0.9			60			60	12
CuOx-Vo [b]	-1.4			63			63	
Ag-Cu$_2$O PS [c]	-1.2		1.7	7.8	20.1			

Mesoporous Cu film [d)]	-0.8						57	7
N-doped graphene dots [d)]	-0.75			31			67	40
Cu DAT wire [d)]	-0.69						68.9	124
Au$_3$Cu [d)]	-0.38	90.2						
Ultrathin Cu/Ni(OH)$_2$ NS [d)]	-0.39	92						
Nanoporous Cu [e)]	-0.67			38.6	16.6	4.5	62	411
ZnO/CuO [e)]	-0.68			18.1	41.4	5.5	66.7	
CuAg wire [e)]	-0.68			60	25		85	265
Surface Reconstructed Cu [f)]	-2.6			56		5	73	17
Abrupt Cu interface [g)]	-0.67						81	608
3D porous hollow fibre copper [h)]	-0.4	72						

As can been seen in the Table 4.1, there are many factors influencing the selectivity and productivity, such us type of metal, surface structure, shape. Basically, to make products with high value, high energy will be required. For example, CO can be produced at a current of ~-0.4V with high production, while approximately -0.7V will be required to produce more valuable carbon chemicals. Though it is very hard to do quantitative analysis due to too many uncertain/various factors, qualitative analysis can be done to further guide experimental or computational study to design and synthesize more reliable Cu-based catalysts. According to the basic knowledge of electrochemistry and the published catalysts in Table 4.1, we may obtain the following summarization.

First, currently, Cu is the most important metal for CO_2 conversion. Scientists studied the shape and the particle size of Cu-based catalysts to produce more efficient catalysts. From the

macro scene, catalysts with high specific surface area are more efficient because they provide more adsorption sites for CO_2 and intermediates, which have been partially proved by the evidences listed in the above table that the abrupt Cu interface has very high current for CO_2 conversion at low potential and most Cu are produced to nanoscale size. At the micro level, it cannot be guaranteed that higher productivity of target product will be achieved when the particle size because smaller. Because too small particle size may result in the shortage of multi-sites to produce products with more than one carbon. This deduction may be supported by Rulle Reske's experiment, showing that the main product will be CO and H_2 when the particle size of the catalyst is smaller than 2 nm.

Second, the doped metal in Cu is significant to determine the final product. Different metal doped in Cu may cause different product preference and the ratio of metals doped in the Cu also influence the product distribution. For one thing, specific metal may increase the current. For another thing, it can improve the adsorption site to avoid the steric hindrance. Basically, Au, Pd, Zn and Ag catalysts favor the formation of CO, which means it is hard to produce products with more value when they are used alone. However, when Au and Ag is doped in Cu, they can reduce the energy cost to produce more valuable products. For example, CuAg wire and ZnO/CuO are excellent catalysts to produce C_{2+} products with high efficiency at relatively low potential, and faradaic efficiency are 85 and 66.7 at -6.8 V, respectively. However, when Pd and Au are doped in Cu, the effect to increase organic carbon chemicals is limited or even counterproductive. The possible reason is that there is competition in the alloy which means Cu may be stronger to absorb CO_2 than Zn and Au, while it is weaker to absorb CO_2 than Pd and Au. Another possible reason is that the atomic radius of doped atom (Pd:169 pm, Au:174 pm,

Ag:165 pm, Zn:142 pm, Cu:145 pm) may not match the bond length of C-C, resulting in blocking C-C formation.

4.2 Mechanism and pathways for CO_2 conversion to C_2 products

Understanding electrocatalytic mechanism and the relationship between catalyst's structure and performance on molecular level will further provide sights and thoughts to design and improve catalysts to enhance CO_2 reduction ability and produce more high-value products. However, proposing a conclusive mechanism for the reduction of CO_2 is challenging, as more than ten chemicals are produced from CO_2. Besides, these chemicals include a broad mix of aldehydes, ketones, carboxylic acids, and alcohols, out of which 12 are C_2 or C_3 species, showing the complexity of this reaction. Therefore, a lot of work have been done to improve the efficiency and selectivity. Though the relationships between catalytic performances and various factors (pH, defect, size, shape, chemical bond, etc.) have been experimentally investigated, most publications have not systematically discussed the reaction pathway and mechanism. As we know, the electron transfer to adsorbate is thought to have low kinetic barrier. The step for achieving C-C coupling determines the rate and selectivity of C_2 products, because it needs to overcome the barrier of C-C bond formation which consumes much energy.

There is nearly no debate that CO_2 will be converted to HCOOH and CO first. HCOOH can not be converted to other chemicals further. Normally, CO is ideal product because it is the intermediate to electrocatalytically produce organic carbon chemicals, such as CH_4, C_2H_4, and CH_3CH_2OH. Experiments also reveal that the product distribution of CO reduction is as same as that of CO_2 reduction. Those are why many researches focus on CO conversion when they study the mechanism of CO_2 conversion.

To obtain more valuable organic carbon chemicals, the first step is to prohibit the formation of HCOOH and the desorption of CO. Since CO and formate products involve very different reaction mechanism, formate formation can be suppressed by controlling pH, designing new nanoscale catalysts and modifying the properties of the electrolyte, to obtain high concentration of CO. Meanwhile, it is found that Cu(100) only leads to CO formation without $HCOO^-$. Ruud Kortlever et al [2] proposed the reaction pathways in Figure 4.1. They pointed out that when the applied potential was -0.8V, the reaction occurred on the Cu(111) facet and the products tended to be C_1 and CH_4 was dominant when *CHO and *COH were the intermediates. When the applied potential was low, reaction occurred on Cu(100) and *CO dimerization occurred on Cu(100) facet to produce C_2 products which was dominated by C_2H_4. Ming Ma et al [3] proposed that there were two pathways to produce C_2 products (Figure 4.2) and C_2H_4 could be produced from both *CO → *COH → C_2H_4 and *CO + *CO → *COCO paths. However, both research only focused on thermodynamic level, ignoring the influence of reaction barriers. For example, though direct dimerization of *CO is thermally available under low potential, it is obvious that the barrier of dimerization of adsorbed *CO is still very high under an electric field and it is unfavorable from kinetic perspective [4].
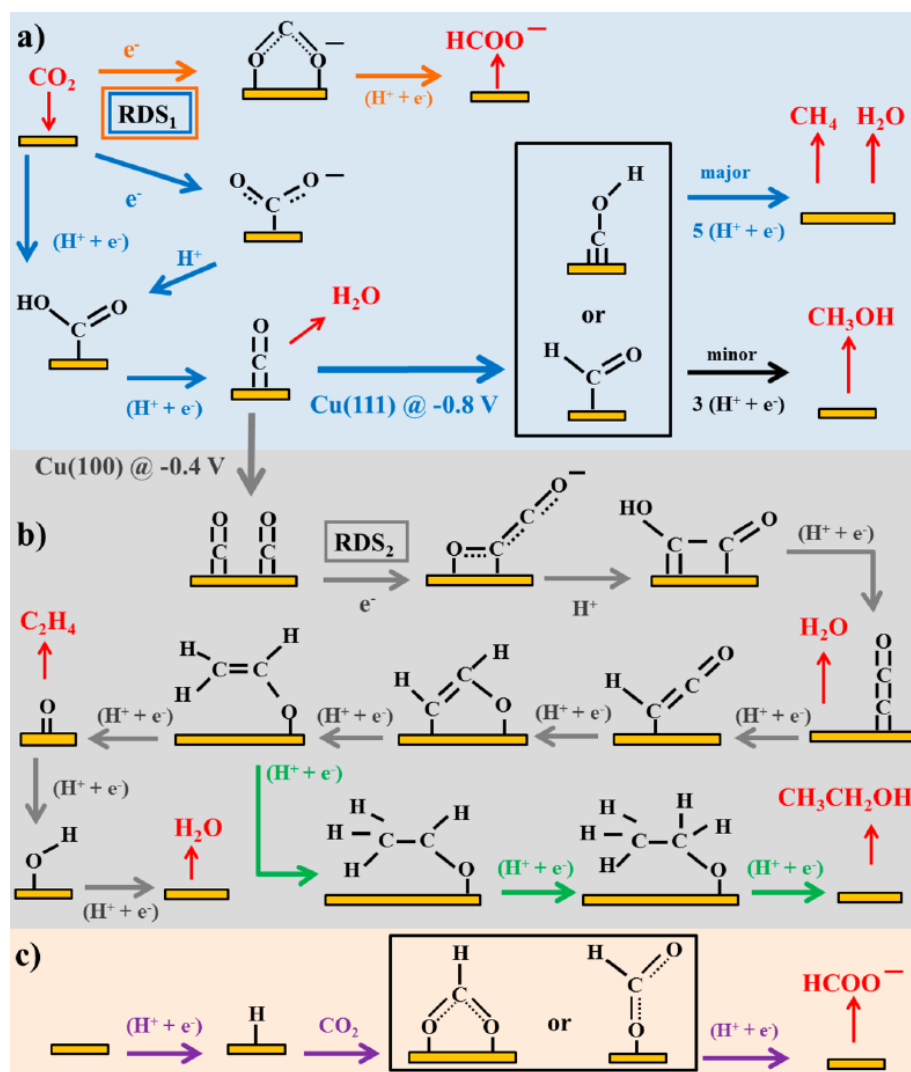
Figure 4.1. Possible reaction pathways for the electrocatalytic reduction of CO_2 to products on transition metals and molecular catalysts [2].
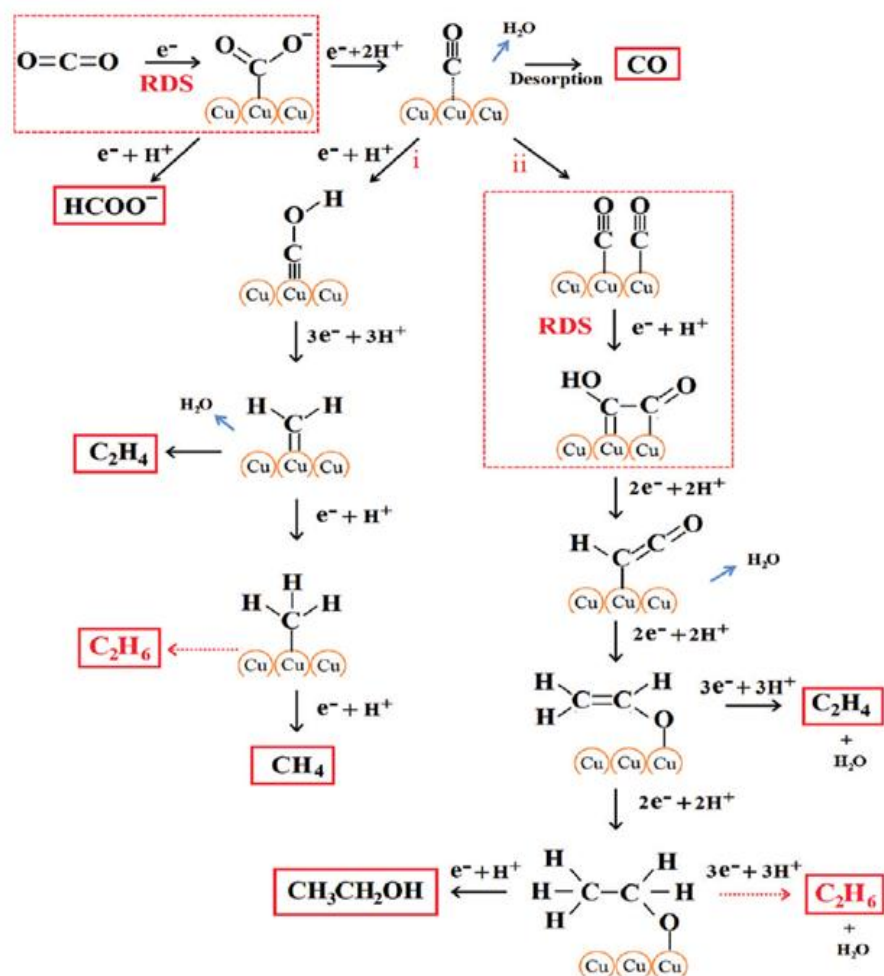
Figure 4.2. Proposed reaction paths for electrocatalytic reduction of CO_2 on Cu nanowire arrays [3].

In 2013, electron-ion transfer reactions were taken into account to study reaction kinetics of elementary steps. The results indicated that the reduction of CO was the key selectivity-determining step on Cu(111) and *COH played a critical role in forming methane/ethylene. C_2H_4 was produced through nonelectrochemical *CH_2 dimerization as shown in Figure 4.3. Moreover, it was further proved that reaction environment and potential were essential for determining intermediates content and the formation of methane/ethylene [5].

Figure 4.3. Proposed reaction paths for CO_2 electroreduction on Cu(111) [5].

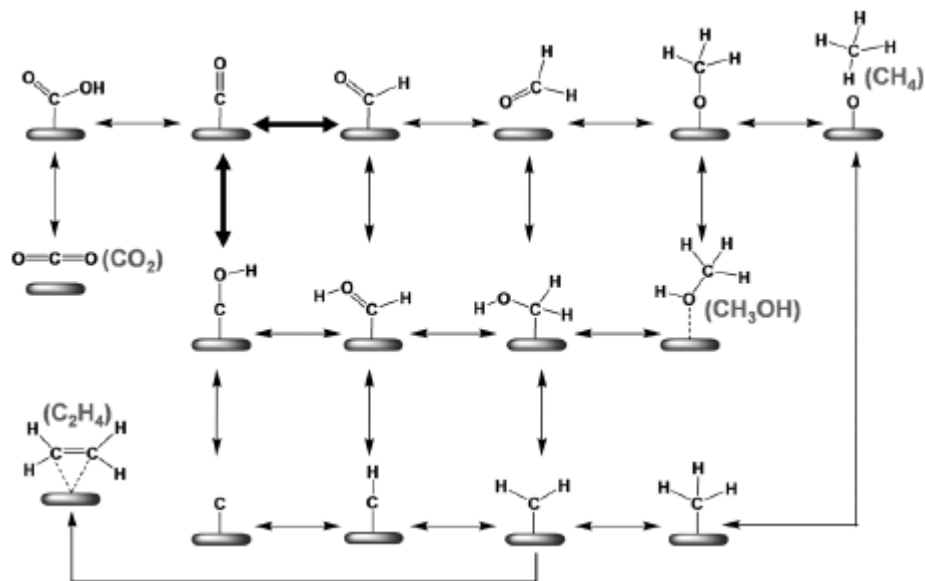In 2016, Xiao et al [6] predicted the atomistic mechanisms for the pathways of products during CO reduction at different pH conditions on Cu(111) facet. Free energies for CO reduction (Figure 4.4) indicated that C_1 products were relatively easy to be produced at acidic atmosphere while C_2 chemicals preferred *CO + *COH/*CHO pathway at neutral pH or *CO + *CO $\rightarrow$ *COCO pathway at alkaline atmosphere. At low pH = 1 with potential of -0.80 V, multi-carbon production was kinetically suppressed, C_1 products were mainly produced through *COH pathway. At neutral pH value with potential of -1.17 V, though both *CO + *CO $\rightarrow$ *COCO and *CO + *COH/*CHO pathways might be accessible, *COH reduction was dominant and C_1 was the man product. At high pH = 12, C_1 pathway was kinetically blocked and *CO + *CO $\rightarrow$ *COCO pathway was predominant. However, we must point out that *COCO is highly unstable on the Cu(111) surface. Compared to *CHO, *COH was favored due to their activation barriers of *COH(0.21 eV) and *CHO(0.39 eV) calculated by DFT at -1.15 V on Cu(111) facet [2].
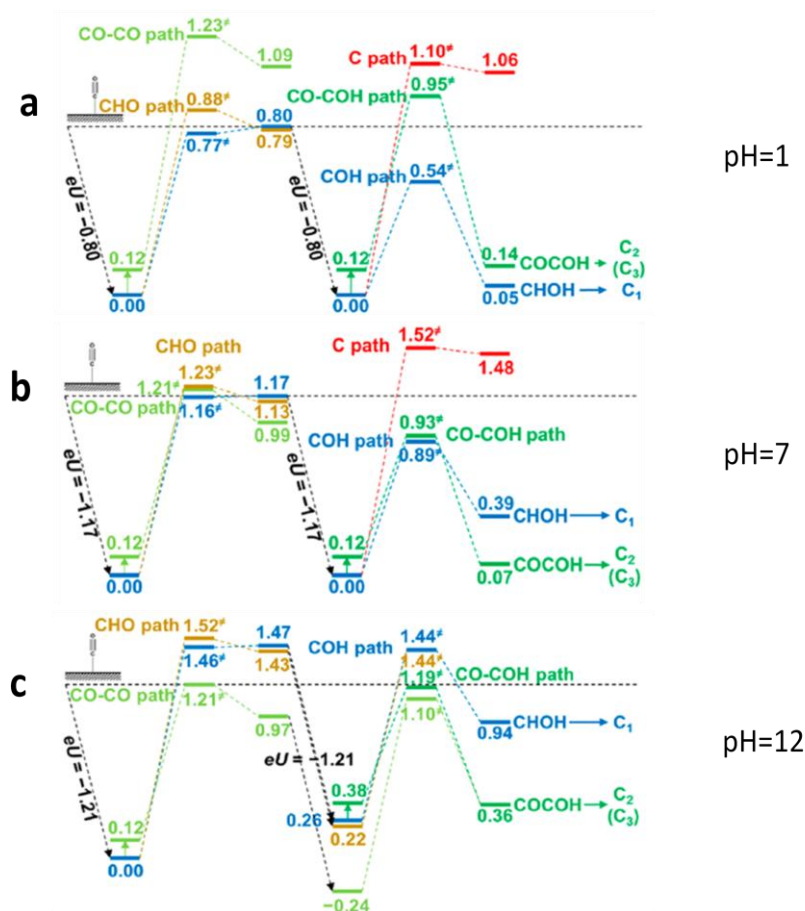
Figure 4.4. Free energy of CO electrochemical reduction on Cu(111) at pH = 1, 7 and 12, respectively [6].

Though Cu(111) facet can be utilized to produce C_1 products and C_2 products, C_1 is preferential. Dimerization of the intermediates *CHO or *COH toward ethylene is believed to be the pathway that produces ethylene once current density reaches 10 mA cm^{-2} and takes place on both Cu(100) and Cu(111) facet. However, Cu(100) is a more active surface than Cu(111), leading to lower overpotentials for both C_1 and C_2 products. Earlier work showed C_1 was preferentially formed on Cu(111), while C_2H_4 was the main product on Cu(100) [9]. In addition, pH value was a significant factor for the product selectivity. At pH = 1 (acidic), CH_4 was observed without C_2H_4 or other C_2 products on both Cu(100) and Cu(111) [7]. In contrast, C_2H_4

production was comparable with CH_4 production in the presence of neutral and basic solutions. As C_2 products was more valuable, reaction on Cu(100) was desirable for its higher performance than Cu(111) to produce C_2 products. Meanwhile, recent experiments showed that under standard electrochemical conditions, Cu(100) may be more stable. In 2015, Tao Cheng et al [8] reported *CHO was the main intermediate for C_1 products on Cu(100), rather than *COH. In 2018, Alejandro Garza et al [10] proposed another reaction pathway for the reduction of CO to C_2 products at high potentials on Cu(100). It showed *CO + *CHO → *COCHO occurred first, and then *COCHO was converted to C_2H_4 or CH_3CH_2OH (Figure 4.5), meaning *CHO was the main intermediate when reaction occurred on Cu(100). Based on the previous research, we try to summarize the possible pathways for CO_2 conversion to C_2 products. Basically, there are four pathways for C_2 formation, which are *CO + *CO → *C_2, *CO + *COH → C_2, *CO + *CHO → C_2 and *COH → *CH_2 → C_2. When the potential is small (~-0.4V), though the reaction thermally follows *CO + *CO → *COCO pathway on Cu(100), it is hard to react due to kinetics barrier [9]. When the potential is high, the reaction mainly follows the path *CO + *COH → C_2H_4 or *COH → *CH_2 → C_2 on Cu(111). On Cu(100) surface at high potentials, *CO + *CHO → C_2 is supposed as the main way to produce C_2. Different reaction pathways for C_2 products are summarized in Figure 4.5.
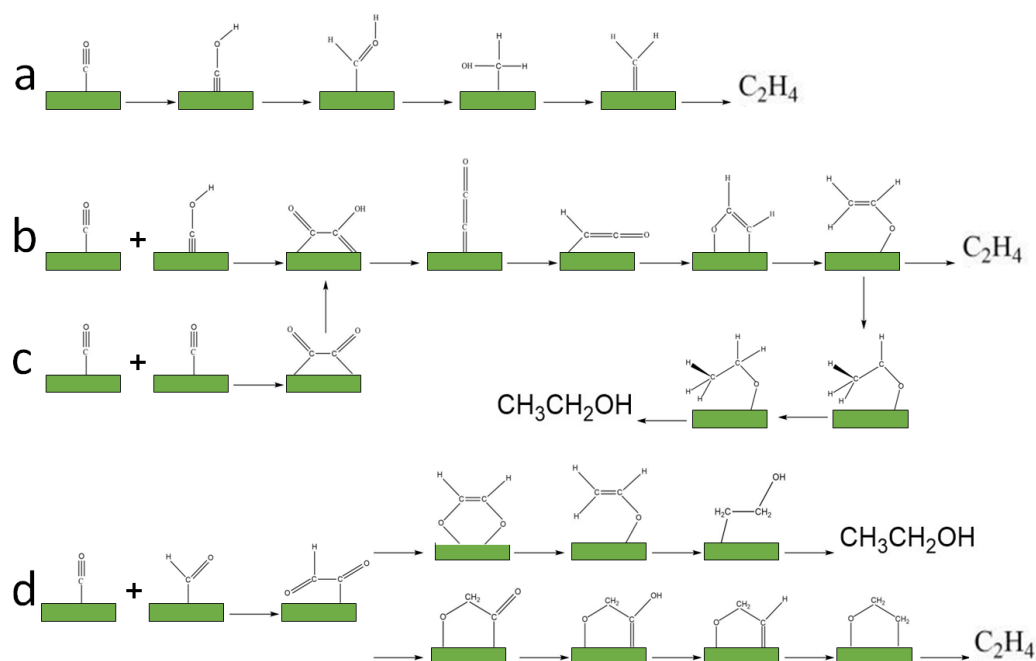
Figure 4.5. Summarized mechanisms for the reduction of CO to C_2 products [1,10].

After we elucidate the reaction mechanism, we can design the effective catalyst to obtain the aimed product. For example, $*C_2H_3O$ is the common reaction intermediate for both ethylene and ethanol formation (Figure 4.5. b, c), therefore, it is possible to modify the catalyst's structure to suppress ethylene production while promote the hydrogenation of the intermediate and finally enhance the selectivity towards alcohols [11,12].

4.3 Conclusion

High overpotential of the reaction and low activity of currently known catalysts still hamper this process from commercialization. Cu-based catalysts are known to electrochemically convert CO_2 to hydrocarbons and/or oxygenates at considerably high faradaic efficiency, however, other products such as CO, HCOO-, and H_2 are also produced at fairly high faradaic efficiencies. The existing catalysts are hard to satisfy the industrial usage (FE >> 50% for C_2 products, current density << −200 mA cm^{-2} while applied potentials >> −1.0 V vs. RHE [8]. In addition, to satisfy the industrial requirements, the catalysts should be durable, however, few research results related to catalyst's lifetime have been reported.

CO_2 can be directly converted to valuable products in the presence of catalyst in one step or two steps which reduced CO_2 to CO first and then converted to fuels with higher energy. This technology can satisfy long-distance and heavy freight transportation requirements. Although CO_2 can be catalytically converted to fuels, it requires high energy. In particular, the reduction of H_2O to H_2 considerably compete with synthesis to fuel at low potential. There is a debate that two steps may be more attractive for lower energy cost and higher selectivity and controllability, because CO reduction activity may be obscured in the presence of a large excess of CO_2 [13]. According to our study, the two step reaction may have more advantages compared with one step reaction [14-17]. On one hand, CO is the intermediate to convert CO_2 to chemical products. Though Cu may be the best catalyst to directly convert CO_2 to organic products, it does not mean it is the best candidate to convert CO_2 to CO. Actually, there are many metals used to produce CO, such as Ag, Au, and Co, most of which achieve the FE more than 90% under relative low potential. On the other hand, the adsorption energy and mechanism of CO on the catalyst surface is significantly different with that of CO_2. The adsorption atom is C for CO adsorption on the

catalyst while O become the adsorption atom for CO_2 adsorption. Compared to CO_2, CO can be easier adsorbed due to its structure. Hence, recently, more and more research are focused on CO conversion.

Current mechanism achievement of converting CO_2 to value-added products are not enough and the debates of reaction pathways are still existing. Because many factors influence the catalyst's performance and it is very hard to build the models to precisely reflect the real situation [18-20]. Though more computational and experimental work need to be done to further elucidate the mechanism of producing C_2 products, the following summaries may be universally accepted.

i) The applied potential is a determining factor influencing the reaction. Though low potential is beneficial, it is impossible to fulfill our goals under certain value. For example, direct dimerization of *CO is thermally available under low potential, it is obvious that the barrier of dimerization of adsorbed *CO is still very high under an electric field and it is kinetically unfavorable. Theoretically, no matter what reaction situation we create, the kinetic barrier exist. At current situation, the range from -0.65 to -1.0 V may be reasonable and acceptable.

ii) Facet is an important factor when we consider the selectivity of CO_2 conversion. Normally, Cu(111) facet prefers to produce C_1 products while Cu(100) facet prefers to convert CO_2 to C_2 products. That is why much research focus on Cu(100) now.

iii) The reaction to produce C_2 products is pH sensitive. C_2 products can be produced with high yield under higher pH value. The situation is corresponding with our former finding that longer nanowire may lead to higher C_2 yield.

iv) It is useful to dope suitable atoms into Cu-based catalysts to change its electrical structure or space structure to further improve the efficiency and selectivity of the catalysts.

v) In reality, making a single proton-electron pair transfer to *CO intermediates to form *CHO/*COH could promote the occurrence probability of coupling to other *CO derived intermediates.

Reference

[1] Yang, Y., Zhang, Y., Hu, J. S., & Wan, L. J. Progress in the Mechanisms and Materials for CO_2 Electroreduction toward C_{2+} Products. Acta Phys.-Chim. Sin. 2020, 36 (1):1-13.

[2] Kortlever, R., Shen, J., Schouten, K. J. P., Calle-Vallejo, F., & Koper, M. T. (2015). Catalysts and reaction pathways for the electrochemical reduction of carbon dioxide. The journal of physical chemistry letters, 6(20), 4073-4082.

[3] Ma, M., Djanashvili, K., & Smith, W. A. (2016). Controllable hydrocarbon formation from the electrochemical reduction of CO_2 over Cu nanowire arrays. Angewandte chemie international edition, 55(23), 6680-6684.

[4] Montoya, J. H., Peterson, A. A., & Nørskov, J. K. (2013). Insights into C-C Coupling in CO_2 Electroreduction on Copper Electrodes. ChemCatChem, 5(3), 737-742.

[5] Nie, X., Esopi, M. R., Janik, M. J., & Asthagiri, A. (2013). Selectivity of CO_2 reduction on copper electrodes: the role of the kinetics of elementary steps. Angewandte Chemie International Edition, 52(9), 2459-2462.

[6] Xiao, H., Cheng, T., Goddard III, W. A., & Sundararaman, R. (2016). Mechanistic explanation of the pH dependence and onset potentials for hydrocarbon products from electrochemical reduction of CO on Cu(111). Journal of the American Chemical Society, 138(2), 483-486.

[7] Liu, X., Schlexer, P., Xiao, J., Ji, Y., Wang, L., Sandberg, R. B., ... & Hahn, C. (2019). pH effects on the electrochemical reduction of $CO_{(2)}$ towards C_2 products on stepped copper. Nature communications, 10(1), 1-10.

[8] Cheng, T., Xiao, H., & Goddard III, W. A. (2015). Free-energy barriers and reaction mechanisms for the electrochemical reduction of CO on the Cu(100) surface, including multiple layers of explicit solvent at pH 0. The journal of physical chemistry letters, 6(23), 4767-4773.

[9] Zheng, Y., Vasileff, A., Zhou, X., Jiao, Y., Jaroniec, M., & Qiao, S. Z. (2019). Understanding the roadmap for electrochemical reduction of CO_2 to multi-carbon oxygenates and hydrocarbons on copper-based catalysts. Journal of the American Chemical Society, 141(19), 7646-7659.

[10] Garza, A. J., Bell, A. T., & Head-Gordon, M. (2018). Mechanism of CO_2 reduction at copper surfaces: Pathways to C_2 products. Acs Catalysis, 8(2), 1490-1499.

[11] Mistry, H., Varela, A. S., Bonifacio, C. S., Zegkinoglou, I., Sinev, I., Choi, Y. W., ... & Cuenya, B. R. (2016). Highly selective plasma-activated copper catalysts for carbon dioxide reduction to ethylene. Nature communications, 7, 12123.

[12] Vasileff, A., Xu, C., Jiao, Y., Zheng, Y., & Qiao, S. Z. (2018). Surface and interface engineering in copper-based bimetallic materials for selective CO_2 electroreduction. Chem, 4(8), 1809-1831.

[13] Li, C. W., Ciston, J., & Kanan, M. W. (2014). Electroreduction of carbon monoxide to liquid fuel on oxide-derived nanocrystalline copper. Nature, 508(7497), 504.

[14]Weng, Z., Jiang, J., Wu, Y., Wu, Z., Guo, X., Materna, K. L., ... & Wang, H. (2016). Electrochemical CO_2 reduction to hydrocarbons on a heterogeneous molecular Cu catalyst in aqueous solution. Journal of the American Chemical Society, 138(26), 8076-8079.

[15] Peterson, A. A., Abild-Pedersen, F., Studt, F., Rossmeisl, J., & Nørskov, J. K. (2010). How copper catalyzes the electroreduction of carbon dioxide into hydrocarbon fuels. Energy & Environmental Science, 3(9), 1311-1315.

[16]Schneider, J., Jia, H., Muckerman, J. T., & Fujita, E. (2012). Thermodynamics and kinetics of CO_2, CO, and H^+ binding to the metal centre of CO_2 reduction catalysts. Chemical Society Reviews, 41(6), 2036-2051.

[17] Savéant, J. M. (2008). Molecular catalysis of electrochemical reactions. Mechanistic aspects. Chemical Reviews, 108(7), 2348-2378.

[18] Lin, S., Diercks, C. S., Zhang, Y. B., Kornienko, N., Nichols, E. M., Zhao, Y., ... & Chang, C. J. (2015). Covalent organic frameworks comprising cobalt porphyrins for catalytic CO_2 reduction in water. Science, 349(6253), 1208-1213.

[19] Montoya, J. H., Peterson, A. A., & Nørskov, J. K. (2013). Insights into C-C Coupling in CO_2 Electroreduction on Copper Electrodes. ChemCatChem, 5(3), 737-742.

[20] Zhu, W., Zhang, L., Yang, P., Hu, C., Dong, H., Zhao, Z. J., ... & Gong, J. (2018). Formation of Enriched Vacancies for Enhanced CO_2 Electrocatalytic Reduction over AuCu Alloys. ACS Energy Letters, 3(9), 2144-2149.